

pyPRISM: A Computational Tool for Liquid-State Theory Calculations of Macromolecular Materials

Tyler B. Martin^{1*}, Thomas E. Gartner III², Ronald L. Jones¹, Chad R. Snyder^{1*}, Arthi Jayaraman^{2,3*}

1. National Institute of Standards and Technology, Gaithersburg MD, 20899
2. Department of Chemical and Biomolecular Engineering, 150 Academy Street, Colburn Laboratory, University of Delaware, Newark DE
3. Department of Materials Science and Engineering, University of Delaware, Newark, DE

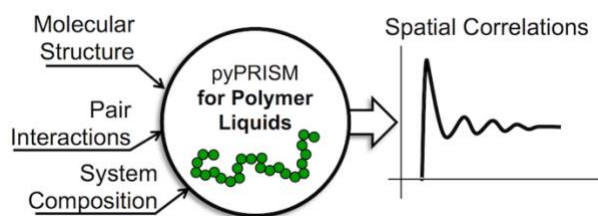
* corresponding authors: tyler.martin@nist.gov, chad.snyder@nist.gov and arthij@udel.edu

OFFICIAL CONTRIBUTION OF THE NATIONAL INSTITUTE OF STANDARDS AND
TECHNOLOGY; NOT SUBJECT TO COPYRIGHT IN THE UNITED STATES

Abstract

The Polymer Reference Interaction Site Model (PRISM) theory describes the equilibrium spatial-correlations of liquid-like polymer systems including melts, blends, solutions, block copolymers, ionomers, liquid crystalline polymers, and nanocomposites. Using PRISM theory, one can calculate thermodynamic (second virial coefficients, Flory-Huggins χ interaction parameters, potentials of mean force) and structural (pair correlation functions, structure factors) data for these macromolecular materials. Here, we present a Python-based, open-source framework, *pyPRISM*, for conducting PRISM theory calculations. This framework aims to simplify PRISM-based studies by providing a user-friendly scripting interface for setting up and numerically solving the PRISM equations. *pyPRISM* also provides data structures, functions, and classes that streamline PRISM calculations, allowing *pyPRISM* to be extended for use in other tasks, such as the coarse-graining of atomistic simulation force-fields or the modeling of experimental scattering data. The goal of this framework is to reduce the barrier to correctly and appropriately using PRISM theory and to provide a platform for rapid calculations of the structure and thermodynamics of polymeric fluids and nanocomposites.

For Table of Contents Use Only



I. Introduction

The use of free and open-source software (FOSS) in the materials science fields allows researchers from across disciplines to pool their cumulative knowledge into *computational tools* that can be collectively constructed, vetted, and distributed. From ångström to micrometer length scales (and beyond) there have been countless examples of success using the FOSS approach for materials modeling, including in density functional theory (*e.g.*, Quantum ESPRESSO¹, ABINIT²), molecular dynamics (*e.g.*, LAMMPS,³ Gromacs,⁴ NAMD,⁵ HOOMD-blue,⁶ DL_POLY,⁷ OpenMD,⁸ OpenMM⁹), self-consistent field theory (*e.g.*, PSCF¹⁰), and finite element modeling (*e.g.*, OOF,¹¹ MOOSE,¹² FEniCS¹³). These codes allow specialists in the chemical, physical, and biological fields access to complex modeling and computational techniques without requiring the detailed programming background necessary to write a codebase from scratch. Furthermore, when these tools are openly and collaboratively developed, they often contain a greater diversity of features and techniques than would be available from a code developed by a single group. Beyond modeling itself, there have been many packages developed to assist in initiating, analyzing, and visualizing the results from the above-mentioned modeling tools (*e.g.*, PACKMOL,¹⁴ Avogadro,¹⁵ GPU RDF calculator,¹⁶ MDAnalysis,¹⁷ VMD,¹⁸ Ovito¹⁹). The success of these efforts in bringing complex modeling and analysis techniques to the broader materials science community motivates theoreticians and simulators to develop their computational materials research techniques into FOSS packages.

The focus of this paper is one such computational technique, Polymer Reference Interaction Site Model (PRISM) theory. PRISM theory describes the liquid-like structural correlations in single and multi-component polymer melts, solutions, nanocomposites, and complex fluid systems. PRISM theory descends from the Reference Interaction Site Model (RISM), which is an

extension of the classical Ornstein-Zernike (OZ) liquid state theory.^{20, 21} While OZ theory is limited to describing atomic fluids, RISM theory was initially developed to study diatomic fluids such as nitrogen, oxygen, and bromine, and later extended to small molecules such as chloroform and acetonitrile.²¹⁻²⁴ RISM (and PRISM) relate various *intra*- and *inter*- molecular correlation functions with so-called ‘closure’ relations, which connect these correlations to pairwise interaction potentials acting between components of the fluid. Together, the RISM/PRISM equations and closures form a set of coupled nonlinear integral equations that allow for structural correlation functions to be calculated. Despite its success for small molecules, RISM theory is not immediately applicable to polymer systems because the conformational flexibility of polymer chains results in a coupling between the *intra*- and *inter*- molecular correlations that makes solving the RISM equations intractable. Furthermore, RISM individually tracks the pair correlations of each site in a molecule, which quickly becomes computationally unfeasible for polymers of even modest chain lengths. PRISM theory initially circumvented these limitations by focusing on dense homopolymer melts, where Flory’s conformational ideality could be naively invoked to effectively ignore the effect of *inter*-molecular correlations on *intra*-molecular correlations and to pre-average correlations between identical site-type pairs.^{25, 26} Since that time, these ideality restrictions have been relaxed *via* the use of more realistic *intra*-molecular correlation functions^{27, 28} and techniques such as self-consistent PRISM.²⁹⁻³³ Using these approaches, PRISM theory has been validated for homopolymer melt systems by comparing predicted structure factors to experimentally derived structure factors from X-ray and neutron scattering.³⁴⁻⁴⁰

Polymer blends have also been extensively studied *via* PRISM theory; this work includes the special case of isotopic blends.^{33, 41-65} While PRISM theory alone cannot predict the structure of macrophase separated blends, it has been used to understand the structure of the mixed phase and

the nature of the spinodal phase transition. Initially, PRISM was shown to incorrectly predict the molecular weight dependence of the blend critical temperature.⁶⁶ This flaw was later remedied by either the introduction of *molecular closures* which more explicitly account for the connectivity between segments of a molecule than atomic closures^{52, 53, 57} or the use of thermodynamic perturbation theory which is valid when the attractive interactions that drive demixing do not significantly perturb local packing structure.^{42, 50, 67-69} For polymer blends, PRISM theory also predicts that the effective interaction parameter, $\chi^{eff}(k)$, has a wavenumber dependence,^{49, 63, 65} a concept which has been seen in some experiments⁴¹ but is debated elsewhere.⁷⁰ In an analogous fashion to blended systems, PRISM theory has also been used to understand the melt structure and microphase separation behavior of random and block copolymer systems in the strongly fluctuating or clustering region of the globally homogeneous phase.^{55, 71-82}

PRISM has also greatly expanded our understanding of the structure and miscibility behavior of polymer nanocomposites^{71, 83-118} and polymer-colloid suspensions.¹¹⁶⁻¹³⁰ For the latter, novel polymer physics-guided closures have been formulated and widely applied. For both these systems, it is of primary interest to understand the spatial structure and phase separation of the particle (filler or colloid) and how polymers statistically organize around the particle. From a structural perspective, PRISM theory predicts the spatial correlations of polymer-particle materials in real- and Fourier-space as pair correlations and structure factors, respectively. This information has been used to describe how the pair interactions in nanocomposites lead to matrix chains wetting and bridging particles in nanocomposites and, in turn, how these phenomena relate to particle dispersion.¹¹²⁻¹¹⁴ Additionally, PRISM theory predicts thermodynamic quantities such as the potentials of mean force, second-virial coefficients, and effective interaction parameters, each of which describe the interactions of these systems. By combining these analyses, PRISM provides a

complete description of the spatial arrangement and thermodynamics of nanocomposite and polymer-colloid systems.

Polyelectrolytes are another important class of materials that have been studied *via* PRISM theory.^{29, 128, 131-150} Simulation methods are challenged to accurately and efficiently represent these systems due to the computational expense of evaluating the long-range electrostatic interactions. PRISM theory circumvents this limitation as the interaction potential need only be computed once at the beginning of the calculation, rather than at every timestep during a simulation. Using PRISM theory, structure factors and osmotic pressures have been predicted for rigid and flexible polyelectrolytes which agree with experiments and simulation.¹³² It is important to note that these successes have been limited to the case of polyelectrolytes in a good solvent, as there are numerical limitations to solving PRISM theory for the bad solvent case.¹³²

Beyond the studies listed above, PRISM theory has also been used to understand systems that involve more exotic architectures, chemistries, or geometries. Examples of new architectures/chemistries include star polymers,^{108, 109, 151-154} comb and sidechain polymers,^{83, 86, 151, 155-161} dendrimers,^{151, 162, 163} ionomers, and ionic-liquids.¹⁶⁴⁻¹⁶⁶ While PRISM theory is typically used as a 1-dimensional, radially symmetric formalism, it has also been extended in a multi-dimensional form so that the orientational structural anisotropy of liquid-crystals and the isotropic-nematic or isotropic-discotic phase transition could be predicted.¹⁶⁷⁻¹⁷⁰ PRISM theory has been applied to understand the adsorption of polymers in slit-like pores and the segregation of physical blends near surfaces in an extended formalism called Wall-PRISM.^{51, 152, 171, 172} By coupling PRISM with other theories, it can extend beyond its basic definition as an equilibrium formalism for isotropic polymer liquids. For example, PRISM has been used with mode-coupling theory to predict the dynamics of polymer melts¹⁷³ and with thermodynamic density functional theory to

study inhomogeneous, phase separated systems.¹⁷⁴⁻¹⁷⁷ These examples demonstrate that PRISM theory is highly flexible in describing a range of soft-matter systems and materials.

In addition to making structural and thermodynamic predictions, PRISM has been applied as a coarse-graining engine to derive simplified force fields from the results of atomistic (or less coarse-grained) simulations.¹⁷⁸⁻¹⁹⁴ Broadly, this approach consists of using non-interacting “ghost” sites to track the global correlations of groups of atoms or sites on a molecule. These group correlations can then be combined with closure relations to derive effective, coarse-grained pair potentials that reproduce the thermodynamics and structure of the more detailed system. One example of this approach is called Integral Equation Coarse Graining (IECG).^{180, 181, 184-188} Despite some questions raised about the thermodynamic consistency of this method, recent work has served to support IECG’s accuracy when used correctly. References 178, 180-183, 185 present detailed discussions on this IECG method and the proof of its thermodynamic consistency. Overall, using PRISM to create coarse-grained representations of polymer systems represents a unique and powerful use of the theory beyond structural and thermodynamic predictions.

Despite these past successes of PRISM theory, overall there are fewer PRISM-based studies compared to simulation techniques such as molecular dynamics or Monte Carlo. One explanation for the reduced number of studies is the lack of an open-source package for PRISM theory. This motivates our efforts described in this manuscript to introduce a user-friendly open-source package for PRISM theory. In this article, we present the theory and initial release implementation of PRISM as a FOSS package called *pyPRISM*. We first present the theoretical formalism for PRISM and its capabilities, then provide an introduction to our coding framework, which is designed to provide a simplified interface for using PRISM.¹⁹⁵⁻¹⁹⁸ The codebase is structured to make the addition of new closures, *intra*-molecular correlation functions, and interaction potentials as

simple as possible so that *pyPRISM* can be easily extended with new features and capabilities. While the initial release of *pyPRISM* focuses on providing a pathway for numerically solving the PRISM equations to produce structural and thermodynamic quantities, the framework is designed to be easily expanded to other applications such as modeling scattering data or coarse-graining detailed molecular simulations.

In the following sections, we will describe PRISM theory in detail, present our implementation of PRISM in the *pyPRISM* package, and review several PRISM-based case studies. These case-studies serve to demonstrate the various uses of PRISM theory to the reader and validate our codebase by comparison to published data. Beyond the GitHub repository which hosts the codebase,¹⁹⁷ we have also created a companion tutorial¹⁹⁶ that not only teaches users how to use *pyPRISM* but also how to reproduce all of the data shown in the Case Studies section. Finally, *pyPRISM* installation and usage instructions, as well as PRISM-related knowledgebase materials are presented on a dedicated documentation website.¹⁹⁵

II. Theoretical Background

Here we provide the necessary details of PRISM theory to describe our implementation in *pyPRISM*. For further details and discussion on the applications of PRISM theory, please refer to References 67, 87, 93, 99, 132, 199, 200, which either review PRISM in general or within specific application domains.

A. PRISM Equation

PRISM theory describes the spatial correlations between spherical sites which represent either an atomic species or some collection of atoms in the molecule (*e.g.*, a monomer or statistical segment of a polymer chain). By carrying out calculations with multiple site types, one can

represent homopolymers with chemically complex monomers, polymer blends, copolymers, nanocomposites, and colloidal solutions. All information about the chemistry and connectivity of these systems is encoded into the pair-interactions and *intra*-molecular correlation functions as will be discussed below.

In general, for a material system that can be represented with n types of sites, the PRISM equation is written in Fourier space as

$$\hat{H}(k) = \hat{\Omega}(k)\hat{C}(k)[\hat{\Omega}(k) + \hat{H}(k)] \quad (1)$$

with $\hat{H}(k)$ being an $n \times n$ matrix with all pair-wise total *inter*-molecular correlation functions (at a given wavenumber, k) as its elements, $\hat{\Omega}(k)$ being an $n \times n$ matrix of the *intra*-molecular correlation functions, and $\hat{C}(k)$ being an $n \times n$ matrix of direct correlation functions between the sites in a fluid. For example, in a system with three types of sites ($n = 3$), labelled as A, B and C, $\hat{H}(k)$ is written as

$$\hat{H}(k) = \begin{bmatrix} \rho_{AA}^{pair} \hat{h}_{AA}(k) & \rho_{AB}^{pair} \hat{h}_{AB}(k) & \rho_{AC}^{pair} \hat{h}_{AC}(k) \\ \rho_{BA}^{pair} \hat{h}_{BA}(k) & \rho_{BB}^{pair} \hat{h}_{BB}(k) & \rho_{BC}^{pair} \hat{h}_{BC}(k) \\ \rho_{CA}^{pair} \hat{h}_{CA}(k) & \rho_{CB}^{pair} \hat{h}_{CB}(k) & \rho_{CC}^{pair} \hat{h}_{CC}(k) \end{bmatrix} \quad (2)$$

in which $\rho_{\alpha\beta}^{pair} = \rho_{\alpha}\rho_{\beta}$, and $\rho_{\alpha}, \rho_{\beta}$ correspond to the site number densities of site types α and β , respectively. Note that throughout this paper, a carat above a symbol (and/or the functional designation (k)) indicates that the corresponding function or matrix is in Fourier space. $h_{\alpha\beta}(r)$ is related to the *inter*-molecular site-site pair correlation function (*i.e.*, radial distribution function), $g_{\alpha\beta}(r)$ by

$$h_{\alpha\beta}(r) = g_{\alpha\beta}(r) - 1 \quad (3)$$

in which r is the distance between sites of type α and β . Note that all spatial *intra*- and *inter*-molecular correlation matrices are, by definition, symmetric with site type pairs, *i.e.*, $h_{\alpha\beta} = h_{\beta\alpha}$.

$\widehat{\Omega}(k)$ represents the *intra*-molecular correlations and is analogous to the form factor from scattering theory. $\widehat{\Omega}(k)$ for a three-component system is written as

$$\widehat{\Omega}(k) = \begin{bmatrix} \rho_{AA}^{site} \widehat{\omega}_{AA}(k) & \rho_{AB}^{site} \widehat{\omega}_{AB}(k) & \rho_{AC}^{site} \widehat{\omega}_{AC}(k) \\ \rho_{BA}^{site} \widehat{\omega}_{BA}(k) & \rho_{BB}^{site} \widehat{\omega}_{BB}(k) & \rho_{BC}^{site} \widehat{\omega}_{BC}(k) \\ \rho_{CA}^{site} \widehat{\omega}_{CA}(k) & \rho_{CB}^{site} \widehat{\omega}_{CB}(k) & \rho_{CC}^{site} \widehat{\omega}_{CC}(k) \end{bmatrix} \quad (4)$$

where $\rho_{\alpha\beta}^{site} = (\rho_{\alpha} + \rho_{\beta})$ if $\alpha \neq \beta$ otherwise $\rho_{\alpha\beta}^{site} = \rho_{\alpha}$. When solving the PRISM equations numerically, $\widehat{\Omega}(k)$ is one of the inputs which describes the connectivity and structure of the molecules. As will be described in detail in Section II.C, $\widehat{\Omega}(k)$ is either specified using one of the many analytical expressions for various chemical and architectural systems (such as Gaussian or Freely-Jointed Chain)^{67, 99, 132, 200} or obtained *via* molecular simulation.

The direct correlation function, $\widehat{C}(k)$, describes *inter*-molecular correlations between sites when many-molecule (beyond pair) effects are removed.²⁰⁰ Unlike \widehat{H} and $\widehat{\Omega}$, $\widehat{C}(k)$ is not scaled by density, and in matrix form is given by

$$\widehat{C}(k) = \begin{bmatrix} \widehat{c}_{AA}(k) & \widehat{c}_{AB}(k) & \widehat{c}_{AC}(k) \\ \widehat{c}_{BA}(k) & \widehat{c}_{BB}(k) & \widehat{c}_{BC}(k) \\ \widehat{c}_{CA}(k) & \widehat{c}_{CB}(k) & \widehat{c}_{CC}(k) \end{bmatrix} \quad (5)$$

where $c_{\alpha\beta} = c_{\beta\alpha}$.

As written, the above equations are general and correspond to any liquid-like system that can be described by three sites (*i.e.*, atom types or coarse-grained beads). Variation of these equations for fewer or greater numbers of site types is achieved by simply modifying the size of the matrix variables. We note that this formalism pre-averages chain-end effects into the global correlations for a given site-type pair. For example, the correlations between sites in a homopolymer chain are identical regardless of whether the sites are in the center or on the end of the chain. While this is, in general, a necessary assumption to make the task of solving the PRISM equations tractable *via*

the reduction of the number of site types, one could introduce “end site types” for systems where explicit treatment of end-effects is important.

B. Closures

While the above equations specify the base PRISM formalism, we need additional equations called closures to numerically solve the PRISM equations for \hat{H} and \hat{C} . Closures provide a mathematical relation between the direct correlation function $c_{\alpha\beta}$, the pairwise interaction potential $U_{\alpha\beta}$, and, often, the total correlation function $h_{\alpha\beta}$. Since the closures include $U_{\alpha\beta}$, it is through these closures that the chemical details of the system are specified. Examples of so-called *atomic* closures include Percus-Yevick (PY), Hypernetted Chain (HNC), Mean-Spherical Approximation (MSA), Martynov-Sarkisov (MS), and Laria-Wu-Chandler (LWC).^{32, 53} There are also “reference” versions of these closures in which we separate the attractive and hard-core portions of the interaction potentials and include a direct-correlation function from a hard-sphere reference system.⁵³ Finally, as mentioned in the introduction, there are *molecular* closures that include *intra*-molecular correlation functions, $\hat{\omega}(k)$, to account for connectivity between sites and correct scaling issues for phase-separating systems such as blends and copolymers.⁵³

The first release of *pyPRISM* includes the three most commonly used closures from liquid state theory: MSA, PY and HNC. Respectively, the MSA, PY, and HNC closures are written in real space as:

$$c_{\alpha\beta}(r) = -\beta U_{\alpha\beta}(r) \quad (6a)$$

$$c_{\alpha\beta}(r) = (1 - e^{\beta U_{\alpha\beta}(r)})(h_{\alpha\beta}(r) + 1) \quad (6b)$$

$$c_{\alpha\beta}(r) = h_{\alpha\beta}(r) - \ln(h_{\alpha\beta}(r) + 1) - \beta U_{\alpha\beta}(r) \quad (6c)$$

in which $\beta = 1/(k_B T)$, with k_B as the Boltzmann constant and T as the temperature. Unfortunately, the above closures are not useful as written when trying to solve the PRISM

equations numerically, because many liquid systems have hard-core interactions which cause $U_{\alpha\beta}$ to diverge at low r , resulting in floating point overflow in a codebase. One way to get around this limitation is to rewrite the closures in terms of a new variable, $\gamma_{\alpha\beta}$ ⁵²

$$\gamma_{\alpha\beta}(r) = h_{\alpha\beta}(r) - c_{\alpha\beta}(r) \quad (7)$$

The various pairs of $\gamma_{\alpha\beta}$ become components of $\Gamma(r)$, an $n \times n$ matrix for a system with n types of sites. For the three-site example used above,

$$\Gamma(r) = \begin{bmatrix} \gamma_{AA}(r) & \gamma_{AB}(r) & \gamma_{AC}(r) \\ \gamma_{BA}(r) & \gamma_{BB}(r) & \gamma_{BC}(r) \\ \gamma_{CA}(r) & \gamma_{CB}(r) & \gamma_{CC}(r) \end{bmatrix} \quad (8)$$

Substituting $\gamma_{\alpha\beta}$, the PY expression becomes

$$c_{\alpha\beta}(r) = (e^{-\beta U_{\alpha\beta}(r)} - 1)(\gamma_{\alpha\beta}(r) + 1) \quad (9)$$

and the HNC

$$c_{\alpha\beta}(r) = e^{\gamma_{\alpha\beta}(r)} e^{-\beta U_{\alpha\beta}(r)} - \gamma_{\alpha\beta}(r) - 1 \quad (10)$$

Now, the exponential portions of these closures converge to zero for hard core potentials rather than diverging. An alternative strategy to rewriting the closures in terms of $\gamma_{\alpha\beta}$ is to assume $h_{\alpha\beta}(r) = -1$ inside the hard core and to separately calculate $c_{\alpha\beta}$ inside and outside the core. This approach avoids the calculation of divergent potentials for overlapping sites while strictly enforcing the hard-core condition. *pyPRISM* currently supports both approaches for handling hard-core potentials. We note that the MSA closure can only be used *via* the second strategy. While we expect that both approaches should yield the same result in general, users may find that there are situations in which one strategy or the other converges to the numerical solution of the PRISM equations more easily.

Based on the assumptions and strategies used in their derivation, each of the above closures has strengths and weaknesses when applied to different types of systems. For example, for atomic

systems the HNC closure is derived from a well-defined free energy functional and reproduces results from the virial equation.²⁰¹ In practice, the HNC closure has been shown to be more accurate than PY when there are Coulomb interactions and when there is large disparity in site diameters, d_α , but it cannot be numerically solved for low-density systems.^{32, 114} Compared to the HNC, the PY closure generally provides more accurate predictions when the pairwise interactions are hard-core and short-ranged, *e.g.* hard-sphere, weakly attractive Lennard-Jones, or Weeks-Chandler-Andersen interactions.²⁰¹ Finally, while the MSA closure is a rather crude approximation, it is superior to both PY and HNC when modeling square-well fluids.²⁰¹ While somewhat outside the scope of this paper and the *pyPRISM* codebase, the MSA closure is also useful as its relative simplicity often allows for analytical solutions to the PRISM equation to be derived for model systems with small numbers of components.²⁰¹

Overall, the process of choosing the best closure for a system of interest is non-trivial, as there is no *one* closure that has superior predictive performance for all systems. *pyPRISM* makes it easy to swap out and test various closures so that the performance of a specific closure can be evaluated by direct comparison to each other and experiments/simulations. Moving forward, we plan to implement other closures, with a focus on molecular closures so that attractive blend and copolymer melt systems will be accessible to *pyPRISM* users. It is also our intention to work towards automating the process of closure selection based on the system inputs as this process is clearly one of the more challenging aspects of using PRISM theory.

C. Intra-Molecular Correlation Function $\hat{\Omega}(k)$

As stated above, $\hat{\Omega}(k)$ describes the connectivity and structure within a single molecule *via* the *intra*-molecular pair correlations. These correlations are typically described in Fourier space where a non-zero value of $\hat{\omega}_{\alpha\beta}(k)$ at a given k corresponds to the degree of *intra*-molecular ordering

over the length scale $\lambda = 2\pi/k$. By definition, site-types that never exist within the same molecules have $\hat{\omega}_{\alpha\beta}(k) = 0$ and are considered to not have *intra*-molecular correlations over any length scale. For linear polymer chains composed of a single type of site, many expressions for $\hat{\omega}_{\alpha\beta}(k)$ exist. For example, a Gaussian chain is represented as

$$\hat{\omega}_{\alpha\beta}(k) = \frac{1 - f^2 - \frac{2f}{N} + \frac{2f^{N+1}}{N}}{(1 - f)^2} \quad (11)$$

where f is defined as $f = \exp(-k^2\sigma^2/6)$, N is the number of monomers in the Gaussian chain, and σ is the characteristic distance unit.²⁸ Similarly, a freely-jointed chain (FJC) is also represented with Equation 11 above, but with f redefined as $f = \sin(kl)/kl$, in which l is the bond length between sites along the chain.²⁸ Attempts to introduce *intra*-molecular excluded volume into the FJC model have yielded the non-overlapping freely-jointed chain.²⁸ For semi-flexible polymers modeled as worm-like chains, $\hat{\omega}_{\alpha\beta}(k)$ is calculated as a function of persistence length using a discrete Koyama distribution.²⁷ Atomistic descriptions such as the ångström-scale Rotational-Isomeric-State (RIS) model have been employed for specific polymers.^{33, 79, 80, 160, 202, 203} As will be shown in Section IV, many of these $\hat{\omega}_{\alpha\beta}(k)$ have similar long-range (low- k) behavior but show large differences in the mid- and short- range correlations. For linear polymer chains, the choice of $\hat{\omega}_{\alpha\beta}(k)$ depends on the level of detail needed at a given length scale and the specific features of a given polymer system, *e.g.*, semi-flexibility.

Analytical expressions for molecules other than linear polymer chains also exist in the literature. For molecules with only one site of a given type (*e.g.*, a bare spherical nanoparticle), $\hat{\omega}_{\alpha\beta}(k) = 1$. Ring polymers can be represented *via* a slight modification to the expression for the linear Gaussian $\hat{\omega}_{\alpha\beta}(k)$.²⁸ For polymer-grafted particles, analytic expressions for the particle-graft

and graft-graft $\widehat{\omega}_{\alpha\beta}(k)$ have been derived for small numbers of grafted chains.^{101, 104-106} The scattering community has also contributed many $\widehat{\omega}_{\alpha\beta}(k)$ as form factors which are used to model the scattering of various systems, *e.g.* worm-like-micelles.^{40, 204-207}

In many cases, analytical expressions for $\widehat{\omega}_{\alpha\beta}(k)$ for a system of interest simply do not exist in the literature. Rather than deriving a new analytical expression, one can simulate a molecule and calculate $\widehat{\omega}_{\alpha\beta}(k)$ using the Debye scattering relation^{202, 208}

$$\widehat{\omega}_{\alpha\beta}(k) = \left\langle \frac{1}{N^{total}} \sum_i^{N_\alpha} \sum_j^{N_\beta} \frac{\sin(k r_{ij})}{k r_{ij}} \right\rangle \quad (12)$$

in which N_α is the total number of sites of type α in each molecule, N_β is the total number of sites of type β in each molecule, $N^{total} = (N_\alpha + N_\beta)$ if $\alpha \neq \beta$ otherwise $N^{total} = N_\alpha$, r_{ij} is the distance between sites i and j , and the angle brackets represent ensemble averaging over uncorrelated snapshots in a simulation trajectory. The Debye approach removes the need for a complicated analytical representation of $\widehat{\omega}_{\alpha\beta}(k)$ and instead allows its determination for any system that can be constructed and sampled in a simulation. The Debye approach is also a foundational part of the self-consistent PRISM method that will be discussed below in Section II.F.

D. 1-D Fourier Transform

Since the PRISM equations are spherically symmetric 1-D functions of k or r , the appropriate transform is the continuous, 1-dimensional sine transform:

$$k \hat{f}(k) = 4\pi \int r f(r) \sin(kr) dr \quad (13)$$

in which $f(r)$ and $\hat{f}(k)$ are generic 1-D spherically symmetric functions. This result can be derived by writing the standard 3-D Fourier transform in Cartesian coordinates, transforming to

spherical coordinates, and integrating out θ and ϕ . To use a “Fast” (*i.e.* FFT) implementation of this continuous sine transform, we need to discretize it. First, we redefine our space variables in terms of discrete, integer indices:

$$r = (i + 1)\Delta r \quad (14)$$

$$k = (j + 1)\Delta k \quad (15)$$

$$\Delta k = \frac{\pi}{\Delta r(N + 1)} \quad (16)$$

where i and j are integers ranging from 0 to $(N-1)$ and Δr and Δk represent the grid spacing in real and Fourier space, respectively. Using these definitions, the continuous sine transform can be rewritten as

$$\begin{aligned} & (j + 1)\Delta k \hat{f}((j + 1)\Delta k) \\ &= 4\pi\Delta r \sum_{i=0}^{N-1} (i + 1)\Delta r f((i + 1)\Delta r) \sin\left(\frac{\pi}{N + 1}(i + 1)(j + 1)\right) \end{aligned} \quad (17)$$

Now defining $F(i)$ and $F(j)$ as the discretized forms of $f(r)$ and $f(k)$, we obtain a type-I discrete sine transform

$$\begin{aligned} \hat{F}_j &= (j + 1)\Delta k \hat{f}((j + 1)\Delta k) = k \hat{f}(k) \\ F_i &= (i + 1)\Delta r f((i + 1)\Delta r) = r f(r) \\ \hat{F}_j &= 4\pi\Delta r \sum_{i=0}^{N-1} F_i \sin\left(\frac{\pi}{N + 1}(i + 1)(j + 1)\right) \end{aligned} \quad (18)$$

It is important to note that when using these equations, the result of the discrete sine transform (\hat{F}_j) must be divided by k to obtain the Fourier-transformed function ($\hat{f}(k)$).

E. Numerical Solution

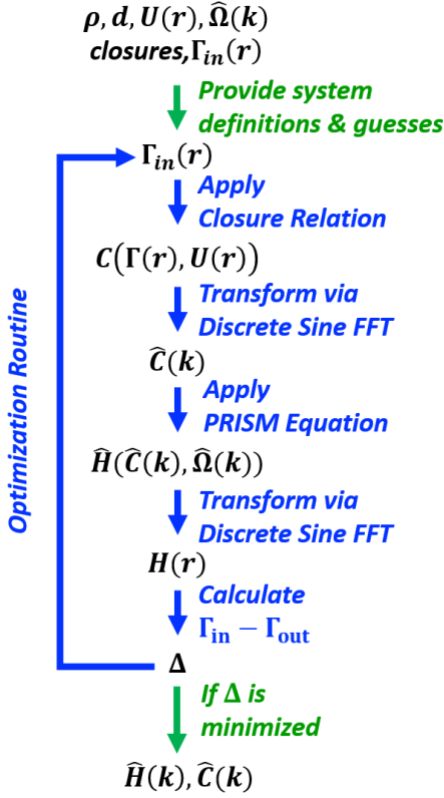


Figure 1: Flowchart of numerical solution methodology. The user defines the system by providing the site densities (ρ_α), site diameters (d_α), inter-site interaction potentials ($U_{\alpha\beta}$), intra-molecular correlation functions ($\hat{\omega}_{\alpha\beta}$), closures for all pairs of site types, and an initial guess for the Γ_{in} values. Using these inputs, the PRISM equations are solved for Γ_{out} and the minimization functional Δ . An optimization routine such as Picard iteration or Newton-Krylov method is applied to minimize Δ to converge the PRISM equations and the resulting \hat{H} and \hat{C} represent valid solutions to the PRISM equations.

In this section, we present the primary approach implemented in *pyPRISM* to solve the PRISM equations, which is also depicted in Figure 1. In this methodology, the equations are numerically solved as follows. First, all site densities (ρ_α), site diameters (d_α), inter-site interaction potentials ($U_{\alpha\beta}$), intra-molecular correlation functions ($\hat{\omega}_{\alpha\beta}$), and closures for all pairs of site types are specified as inputs. These parameters determine the structure and physical interactions of the molecules and are fixed throughout the process of numerically solving the PRISM equations. Next,

a guess provided for $\Gamma_{in}(r)$ is used to calculate $C(r)$ via the chosen closures for each pair. The guess for $\Gamma_{in}(r)$ can be a) set to $\Gamma_{in}(r) = 0$, b) a converged solution of the system at a condition close to the condition of interest, or c) some other arbitrary choice of $\Gamma_{in}(r)$. Once $C(r)$ is calculated and inverted to Fourier space as $\hat{C}(k)$, the PRISM equation (Equation 1) is used to calculate $\hat{H}(k)$ which is inverted back to $H(r)$. Using this $H(r)$ and $C(r)$, $\Gamma_{out}(r)$ is calculated using Equation 7. Then, the output of the minimization function, $\Delta(r)$ is calculated as

$$\Delta(r) = r(\Gamma_{out}(r) - \Gamma_{in}(r)) \quad (19)$$

At this point the choice of solution scheme used to update Γ_{in} based on Δ is up to the user, but the current implementation of *pyPRISM* uses a Newton-Krylov based approach by default.²⁰⁹ Once Δ is minimized to a satisfactory value, the PRISM equations are “solved” and the values for $H(r)$ and $C(r)$ represent solutions to the PRISM equation for the given input parameters.

F. Self-Consistent PRISM

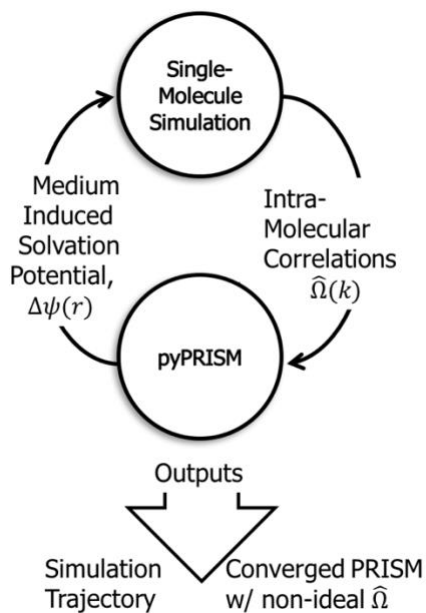


Figure 2: Flowchart of self-consistent PRISM method. The self-consistent loop can either be started by running single-molecule simulations with $\Delta\psi(r) = 0$ or by starting with an ideal expression for $\hat{\Omega}$ and conducting the PRISM calculation.

As mentioned above, one of the original weaknesses of PRISM theory for flexible polymers was the neglect of explicit feedback coupling between the *intra*- and *inter*-molecular correlations. A powerful approach that circumvents this limitation is the self-consistent PRISM (SCPRISM) method.^{29-35, 38, 39, 43, 73, 90, 93, 94, 96, 97, 100, 133, 139, 142, 210-215} In this method, a simulation of a single-molecule of interest is run in the presence of a pairwise-decomposed, medium-induced solvation potential field, $\Delta\psi_{\alpha\beta}(r)$, which is calculated from PRISM theory. The form of the solvation potential depends on the choice of closure used for sites α and β , for the PY and HNC closures the relevant expressions are

$$\beta\Delta\hat{\Psi}^{PY}(k) = -\ln\left(1 + \hat{C}(k)\hat{S}(k)\hat{C}(k)\right) \quad (20)$$

$$\beta\Delta\hat{\Psi}^{HNC}(k) = -\hat{C}(k)\hat{S}(k)\hat{C}(k) \quad (21)$$

in which $\Delta\Psi$ represents the matrix form of the solvation potentials, which are inverted back to real space before use. $\hat{S}(k)$ is the structure factor matrix defined by

$$\hat{S}(k) = \hat{H}(k) + \hat{\Omega}(k) \quad (22)$$

This simulation samples the conformations of the single molecule with the effect of the medium (*e.g.*, solvent, polymer matrix) being introduced *via* $\Delta\psi_{\alpha\beta}(r)$. As the solvent or other chains are not simulated explicitly, these single-chain or single-molecule simulations are much cheaper and more efficient than computationally intensive molecular dynamics or Monte Carlo simulations of the complete system (*e.g.*, multiple chains at the desired concentration). Using the trajectories from these single-molecule simulations, $\hat{\omega}_{\alpha\beta}(k)$ is calculated using the Debye equation (Equation 12) and used as input for a PRISM calculation. The PRISM equations are then solved and the resultant $\hat{C}(k)$ and $\hat{S}(k)$ are then used to recalculate $\Delta\psi_{\alpha\beta}(r)$, which is fed back to a new simulation, thereby completing the self-consistent loop. The calculation loop continues until a convergence criterion or criteria is/are satisfied. For example, for the specific system presented in the work by

Nair and Jayaraman and for the specific convergence criteria they used, converged solutions were obtained within approximately 5 iterations.⁹³ The convergence criterion used by Nair and Jayaraman was

$$SSE_{n \rightarrow n+1} = \sum_{\alpha, \beta} \sum_r \left(\Delta\psi_{\alpha\beta}^{n+1}(r) - \Delta\psi_{\alpha\beta}^n(r) \right)^2 \quad (23a)$$

$$\frac{SSE_{n \rightarrow n+1}}{SSE_{0 \rightarrow 1}} \leq 0.001 \quad (23b)$$

in which n denotes the n^{th} self-consistent iteration and $\Delta\psi_{\alpha\beta}^n(r)$ is the solvation potential of the n^{th} iteration. The number of iterations any user may need will depend on the system and the convergence criterion. The result of the self-consistent method is not only a PRISM calculation where non-ideal conformation effects are explicitly included, but also single-molecule trajectories with mean-field medium effects. The self-consistent PRISM-simulation approach explicitly includes the coupling between the *intra*- and *inter*-molecular correlation functions *via* the self-consistent construction of the method. *pyPRISM* is currently fully capable of being used in the SCPRISM format, although users will have to code their own linkage between their simulation of choice and *pyPRISM*. Future versions of *pyPRISM* will include utilities to assist in the calculation of $\widehat{\omega}_{\alpha\beta}(k)$ from molecular simulation trajectories using the Debye method, along with other tools for setting up self-consistent PRISM calculations with common simulation packages.

III. Implementation

pyPRISM is written as a Python library (compatible with both 2.7 and 3.5+ series) and currently only depends on two standard numerical computing packages: *Numpy* and *Scipy*.¹⁹⁸ *Numpy* provides a highly efficient array and matrix interface along with optimized linear algebra routines.²¹⁶ Beyond the FFT support as described above, *Scipy* also provides a suite of numerical

optimization classes and functions which are used to numerically solve the PRISM equations.²⁰⁹,

217

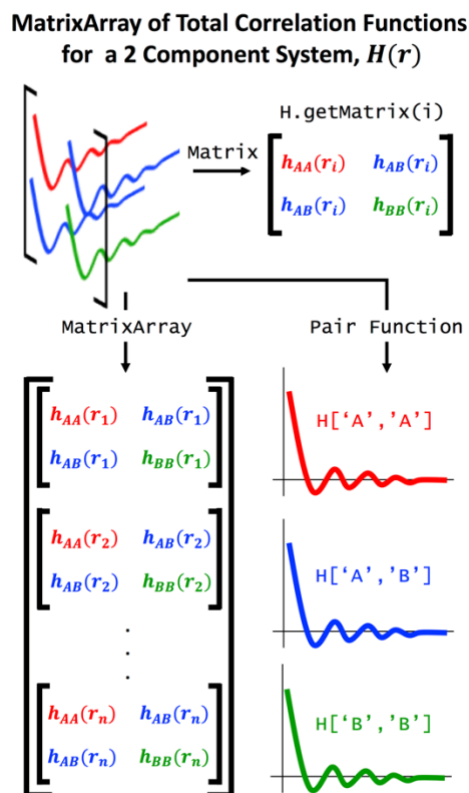


Figure 3: Schematic depiction of a `pyPRISM MatrixArray`.

While a detailed discussion of the object-oriented design of `pyPRISM` is outside the scope of this publication, we wish to highlight our implementation of the `pyPRISM.MatrixArray`, as it is this data-structure that elevates `pyPRISM` from being a “PRISM-code” to a “PRISM-framework”. A schematic depiction of a `MatrixArray` is shown in Figure 3. The goal of this data structure is to provide a unified syntax for both matrix and 1-D function-based mathematical manipulations. For example, while the PRISM equations are solved as a matrix equation (Equation 1), switching between Fourier and real representations of the correlation functions (*i.e.* $\hat{h}_{\alpha\beta}(k) \rightarrow h_{\alpha\beta}(r)$) must

be handled as 1-D pair functions. The `pyPRISM.MatrixArray` data structure transparently and efficiently handles this process by defining common mathematical operations (addition, subtraction, matrix inversion, matrix multiplication, etc.) as operators that broadcast operations across all matrix elements of the array. See Figure 4 for an overview of the available operations. Also in Figure 4, we show how the normalized structure factor matrix with elements defined by

$$\rho_{\alpha\beta}^{site} \hat{S}_{\alpha\beta}(k) = \rho_{\alpha\beta}^{pair} \hat{h}_{\alpha\beta}(k) + \rho_{\alpha\beta}^{site} \hat{\omega}_{\alpha\beta}(k) \quad (24)$$

can be calculated using two `MatrixArrays`.

```

1 domain = pyPRISM.Domain(*args) # domain discretization
2 W = pyPRISM.MatrixArray(*args) # omega correlation function
3 H = pyPRISM.MatrixArray(*args) # total correlation function
4 rho = pyPRISM.Density(*args).site # site-density matrix
5 x = 1 # scalar value
6
7 # MatrixArray by Scalar Operations
8 ## All matrices in W are modified by the scalar x
9 W*x; W-x; W*x; W/x; # elementwise operations
10
11 # MatrixArray by Matrix Operations
12 ## All matrices in W are modified by the matrix rho
13 W+rho; W-rho; W*rho; W/rho; # elementwise operations
14 W.dot(rho) # matrix multiplication
15
16 # MatrixArray by MatrixArray Operations
17 ## Operations are matrix to corresponding matrix
18 W+H; W-H; W*H; W/H; # elementwise operations
19 W.dot(H) # matrix multiplication
20
21 # Fourier Transformations
22 W_AA = domain.to_real(W['A','A']) # transform one function
23 domain.MatrixArray_to_fourier(H) # transform all functions
24
25 # Other Operations
26 W.invert() # invert each matrix in W
27 W['A','B'] # set or get function for pair A-B
28 W.getMatrix(i) # get matrix i in MatrixArray
29 W.itercurve() # iterate over all 1-D functions
30
31 # Example: Calculation of Structure Factor
32 S = (W + H)/rho
33 S_AB = S['A','B'] # extract S_AB from MatrixArray

```

Figure 4: Code block demonstrating `MatrixArray` mathematics and calculation of normalized structure factor. We note that the example does not show how the PRISM equations are solved, or how \hat{H} , $\hat{\Omega}$, and ρ^{site} are filled with data.

In Figure 4, S , H , and W are `MatrixArrays` representing the structure factor, total correlation function, and *intra*-molecular correlation function ($\hat{\Omega}$) matrices and rho is an $n \times n$ *Numpy* array of site densities. Individual 1-D functions in the `MatrixArray` can easily be extracted and set *via* simple array access operators as shown. Internally, all data in a `MatrixArray` is stored in a three-

dimensional *Numpy* array, which is hidden from the user and relays many linear algebra operations to optimized LAPACK and BLAS libraries and furthermore minimizes memory copying during these operations.

While a PRISM-code might only be designed to solve the PRISM equations for a predefined set of quantities, *MatrixArrays* are designed to simplify the mathematics of PRISM theory in general. In this way, we envision the *pyPRISM* codebase being used as a starting point, *i.e.* a framework, for many types of polymer-liquid state theory tasks. This might include fitting experimental scattering results or coarse-graining atomistic simulation models. Overall, the *MatrixArray* and other data structures in *pyPRISM* reduce the barrier to using PRISM by allowing users to efficiently carry out calculations in a format that is similar to the written mathematics of the literature.

IV. Case Studies

To demonstrate the utility of the *pyPRISM* tool, we now explore several case studies on polymer systems commonly studied using PRISM theory. In each case, *pyPRISM* predicts the real and Fourier space correlations, effective interactions, and thermodynamics of these complex systems as a function of molecular architecture and pair interactions. In all cases, we will also include data extracted from the literature to verify that our implementation of PRISM theory reproduces past PRISM results/predictions. A detailed discussion of the physics underlying these results is not the goal of this paper; we refer the reader to the cited references for comprehensive understanding of the respective systems. See the companion *pyPRISM* tutorial for detailed explanations of how these data are produced using the *pyPRISM* package.¹⁹⁶

A. Homopolymer Melts

One of the classic applications of PRISM theory is to study homopolymer melts; PRISM has been extensively compared to computer simulations, X-ray scattering, and neutron scattering for many olefinic and non-olefinic homopolymer melt systems.^{34-39, 67, 211, 218-220} When the self-consistent PRISM formalism is used, reasonable qualitative but not quantitative agreement is found between these methodologies and measurements. Some of the deviations between atomistic molecular dynamics simulations and self-consistent PRISM theory have been traced to the inability of PRISM to handle angular correlations in liquids.⁶⁷ In these studies it was also shown that, while using the self-consistent version of PRISM theory is a good strategy to decouple the *intra*- and *inter*-molecular correlations, the mean-field treatment of the medium-induced solvation potential is imperfect when compared to detailed atomistic simulations.³⁸ Also within the scope of polymer melts, several studies have explored the solubility of penetrant species *via* estimating Hansen solubility parameters from the cohesive energy density calculated from PRISM theory.^{38, 67, 221, 222} Reasonable agreement between theoretical and experimental solubility parameters has been found for various polyolefins although the PRISM results tend to under-predict experimental values.^{38, 67}

In addition to atomistically-detailed models for specific chemistries, PRISM theory has been used with coarse-grained representations of homopolymer chains. In Figure 5, we show a Kratky plot of $\hat{\omega}$ for five analytical polymer chain models which are currently implemented in *pyPRISM*. This figure highlights the differences between scattering models over long and moderate length-scales. All models reproduce Gaussian chain statistics at long length scales ($k\sigma < 0.5$), but diverge from one another at moderate $k\sigma$. At shorter length scales and higher $k\sigma$ (not shown), the $\hat{\omega}(k)$ converge into two groups: those that include a length scale associated with the bond length (freely-jointed chain, non-overlapping freely-jointed chain, and discrete Koyama) and those that do not

(linear and cyclic Gaussian). Out of all the chain models shown, the discrete Koyama $\hat{\omega}(k)$ best reproduces the simulation data for a standard coarse-grained bead-spring polymer (molecular dynamics, red triangles) at long and moderate length scales; this is expected as it has the most realistic local structure. The discrete Koyama $\hat{\omega}(k)$ was derived to model a semi-flexible worm-like chain and can be calculated for varying chain length and persistence length.²⁷

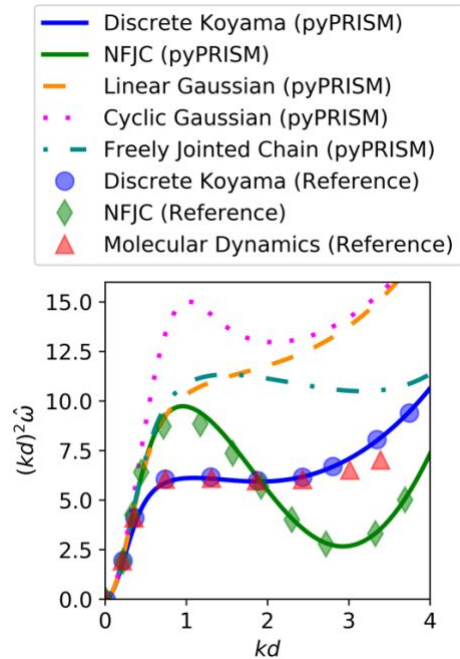


Figure 5: Wavenumber-scaled intra-molecular correlation function, $(kd)^2 \hat{\omega}$, versus the dimensionless wavenumber, kd , showing analytical polymer $\hat{\omega}$ currently implemented in *pyPRISM*. The reference data for the discrete Koyama, non-overlapping freely-jointed chain (NFJC), and molecular dynamics $\hat{\omega}$ are from Figure 2 in Ref. 27. To match these reference data, we use $d = \sigma_{LJ}$ from Ref. 27 in scaling the axes. The details of how these data are generated using *pyPRISM* can be found in the companion *pyPRISM* tutorial.¹⁹⁶

Each of the $\hat{\omega}$ in Figure 5 are implemented in *pyPRISM* as simple Python classes, and new $\hat{\omega}$ are easily added by copying and modifying these classes. It is also important to remind the reader that they are not limited to these analytical $\hat{\omega}$ and that $\hat{\omega}$ can be calculated from simulation using the Debye method outlined in Section II.C.

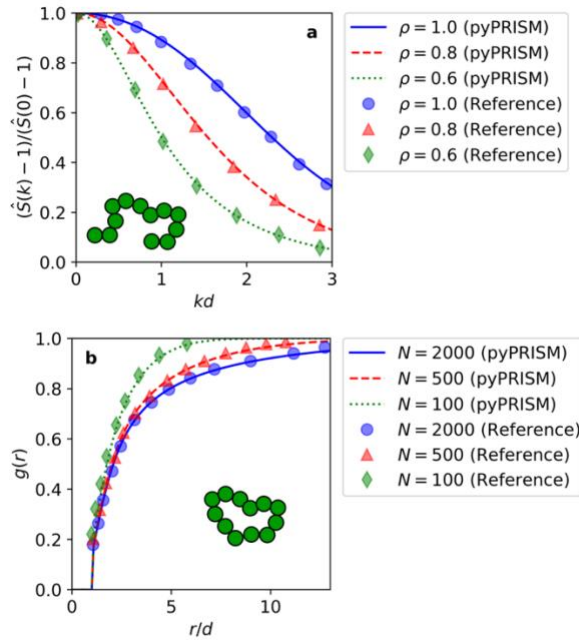


Figure 6: a) Shifted and normalized monomer-monomer collective structure factor, $\frac{\hat{S}(k)-1}{\hat{S}(0)-1}$, versus reduced wavenumber, kd , prediction for a Gaussian, linear homopolymer melt of length, $N=16\,000$, as a function of melt density, ρ , as described in Figure 3 of Ref. 223. b) Monomer-monomer pair correlation functions, $g(r)$, versus reduced separation distance, r/d , of a Gaussian ring-polymer melt at reduced density, $\rho d^3 = 0.9$, with varying chain length, N , from Figure 2 of Ref. 26. The lines are the predictions from pyPRISM and the symbols are data extracted from the corresponding referenced literature. In both subplots, $d = 1.0$ is the characteristic length scale of the system equal to the monomer site diameter. The details of how these data are generated using pyPRISM can be found in the companion pyPRISM tutorial.¹⁹⁶

Figure 6 reproduces PRISM predictions for linear (Figure 6a) and cyclic (Figure 6b) polymer melts. Figure 6a shows the shifted, normalized collective structure factor of linear Gaussian polymer chains in a melt as a function of melt density. The slope of the data is inversely related to a correlation length over which the total density fluctuations decay; this correlation length increases with increasing density. These data smoothly decay with k , rather than tracking local monomer density fluctuations, due to the Gaussian $\hat{w}(k)$ used which does not account for intramolecular excluded volume. While the Gaussian chain assumption has been shown to be

reasonable for ideal, dense polymer melts, with *pyPRISM* we could easily have substituted the Gaussian \hat{w} for one of the others discussed in Figure 5. The system described in Figure 6b is also a homopolymer melt, but the architecture of the chains is *cyclic* rather than *linear*. In PRISM, switching from linear to cyclic polymers is achieved simply by swapping the linear Gaussian $\hat{w}(k)$ for a ring Gaussian $\hat{w}(k)$.²⁶ We note that this ring Gaussian $\hat{w}(k)$ is simply a toy-model for demonstration as modern simulations have shown that ring polymers are collapsed and non-Gaussian.²²⁴ In addition to the Fourier and real-space pair correlation functions shown above, once the PRISM equations are solved for $H(r)$ and $C(r)$, a variety of structural and thermodynamic calculations can easily be calculated, such as isothermal compressibilities²⁷ and equations of state.^{225, 226} *pyPRISM* makes this process simple by codifying these $\hat{w}(k)$ and calculations in simple functions and classes. This highlights the power of PRISM in surveying the effect of molecular architecture in polymer and soft matter systems with minimal user effort and minimal use of computational resources.

B. Polymer Nanocomposites (PNCs)

There have been many PRISM-based theoretical studies focused on understanding how the design of the filler and matrix material in polymer nanocomposites (PNCs) lead to controlled morphologies and particle/filler dispersion in the matrix; much of this work is summarized in several recent reviews.^{87, 93, 99} Due to the nature of the formalism itself, PRISM is uniquely suited to the task of connecting the statistical pair correlations and interactions of the PNC components in the globally disordered or amorphous material state to the resultant PNC morphology. Simulation methodologies are challenged to equilibrate large PNC systems with long matrix chains because the relaxation times of these systems are often much longer than comparable simulations at lower densities and/or with short matrix chains. Results from PRISM calculations are, by

definition, equilibrium predictions, meaning that relaxation times and equilibration are not a problem. Furthermore, the problem of finite-size effects is not present in PRISM theory.

The primary challenge of using PRISM theory to study PNCs is that it cannot predict the behavior of the phase-separated state, *i.e.*, the *aggregated morphology*. This is particularly a problem at higher filler loadings where, even in the mixed state, the filler material can begin to order and crystallize. Often, attempting to use PRISM theory for systems or states where it is not applicable results in numerical convergence issues, but occasionally PRISM will produce non-physical predictions instead. In the former case, it is often unclear whether the lack of convergence is due to numerical limitations or the lack of a true solution due to phase separation. Since understanding the physical and chemical origins of phase separation in PNCs is of primary interest, strategies must be employed to study PNC phase separation without directly doing calculations for phase separated systems. While the standard approach for calculating spinodal phase boundaries with PRISM theory is to observe the divergence of the total collective structure factor at zero wavenumber at the phase boundary is approached,⁵⁹ one can also employ approaches that avoid directly calculating the phase boundary at all. For example, one can infer phase behavior of a PNC system by analyzing the filler-filler potential of mean force. Alternatively, one can focus on systems where attractive particle-matrix interactions stabilize the dispersed morphology. Both strategies are demonstrated below. A secondary challenge is that polymer PNCs often have components with disparate size scales, *e.g.*, large spherical fillers, which make solving the PRISM equations more difficult. This contrasts with polymer melts and blends where the site diameters are often close in value between site types.

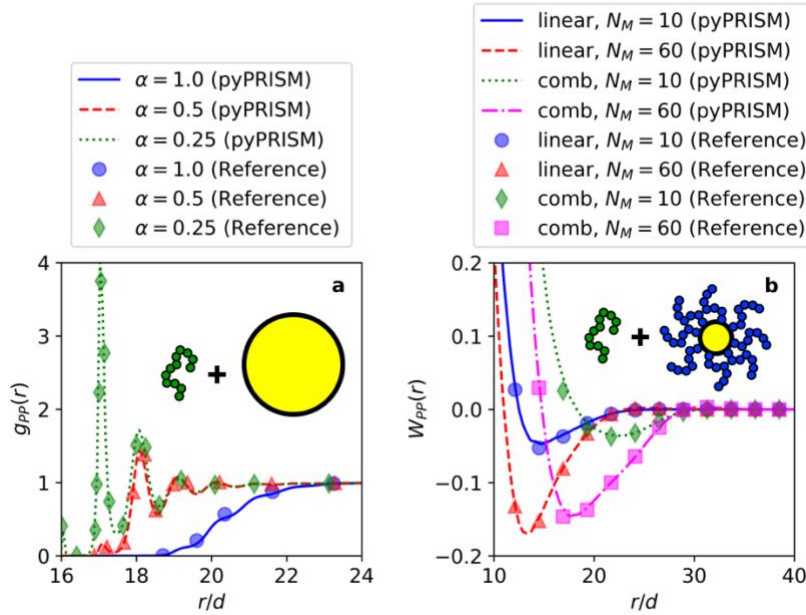


Figure 7: a) Particle-particle site-site pair correlations, $g_{PP}(r)$, versus reduced separation distance, r/d , in a PNC at a total packing fraction, $\eta = 0.4$, with a freely-jointed chain matrix of length, $N = 100$, with attractive polymer-particle interactions at an attraction strength, $\varepsilon = 1.0$, and with varying interaction range, α , as described in Figure 3 of Ref. 113. b) Particle-particle potential of mean force, $W_{PP}(r)$, versus reduced separation distance, r/d , between polymer grafted particles in a linear polymer matrix at a total packing fraction of $\eta = 0.35$ for varying graft architecture and matrix length, N_M , as discussed in Figure 9 of Ref. 83. The lines are the predictions from pyPRISM and the symbols are data extracted from the corresponding referenced literature. In both subplots, $d = 1.0$ is the characteristic length scale of the system equal to the monomer site diameter. The details of how these data are generated using pyPRISM can be found in the companion pyPRISM tutorial.¹⁹⁶

Figure 7a and 7b both describe nanocomposite systems with varying interactions and chain architectures. In Figure 7a, we show the particle-particle pair correlation functions for a system of matrix chains with spherical hard nanoparticles of diameter $D=16d$ (*i.e.*, 16 times the monomer site diameter, d); we note that PRISM theory has also been used to study fillers of diverse non-spherical shapes.^{85, 98} In addition to the heterogeneity in size scales, this example also demonstrates pyPRISM's ability to handle heterogeneous interaction potentials; in this system the hard sphere potential describes pairwise interactions for all species, excepting particle-polymer interactions which are modeled *via* an exponential attraction.¹¹³ It is the particle-polymer attraction that

stabilizes the dispersed state in this system and makes the PRISM calculation possible. The data in Figure 7a show how the ordering of the particles shift as the range of the attractive potential is varied. By analyzing the polymer-particle correlations (not shown), the changes in the particle-particle correlations can be shown to be a result of complex surface wetting and particle-particle bridging behavior of the matrix chains. PRISM tracks the density fluctuations of all components over all length scales so that information about relative locations of various species can easily be determined as a function of interaction parameters.

In contrast to the example in Figure 7a, the PNC system in Figure 7b has athermal interactions for all pairs of sites and has polymer chains permanently grafted to the particle surface. The purpose of these grafted chains is to tune the dispersability of the particles as a function of graft length and architecture. These calculations are conducted at infinite dilution of polymer grafted particles to calculate the effective particle-particle interactions, which can be analyzed to understand the dispersibility. In this case, analytical expressions for the graft-particle and graft-graft $\hat{w}(k)$ do not exist and these functions are calculated using the Debye approach and short simulations of a single grafted particle. As is shown by the shift of the minima of the potentials of mean force, PRISM captures the effect of varying chain length as a wetting-dewetting effect. This wetting-dewetting effect is connected to the graft to matrix chain length ratio which dictates the mixing-demixing of the graft and matrix chains and, in turn, the macrophase separation of the PNC.⁹⁹ Furthermore, Figure 7b also demonstrates the power of the Debye approach, which allows us to make predictions for systems with complex comb-polymer architectures that do not have analytical expressions for $\hat{w}(k)$.⁸³

C. Block copolymers

Another important class of systems that has been studied *via* PRISM are block copolymers. PRISM has been applied to understand the thermodynamic and structural implications of block architecture, sequence, and composition in a variety of copolymer melts and solutions.^{72, 75-82, 227} For example, PRISM was used to demonstrate how the effective Flory-Huggins χ parameter (one of the many potential thermodynamic outputs of a PRISM calculation) and the peak scattering intensity in a block copolymer melt varied as a function of multiple parameters including temperature, chain length, composition, stiffness asymmetry, and others.⁷⁷⁻⁸¹ In later work, structural quantities and estimates for the microphase spinodal temperature for copolymer solutions were studied as a function of temperature, chain length, and copolymer concentration.^{76, 227} Despite these and many other successful applications of PRISM theory to block copolymers, there are several challenges associated with these systems. First, as described with polymer blends in Section IIB, *molecular* closures (rather than *atomic* closures) are in general necessary for accurately determining key thermodynamic and structural properties due to effects of the chain connectivity on the spatial correlations which are not accounted for in the *atomic* closures.^{52, 53, 80} This requirement increases the complexity of implementing and solving the PRISM formalism. Additionally, phase-separated systems cannot be directly accessed with PRISM, rather, information about the phase transition and phase-separated structure must be inferred from the properties of the disordered state. Finally, due to the vast array of chain architectures, compositions, sequences, and chemistries that can be synthetically incorporated into block copolymers, analytical $\hat{w}(k)$ are unlikely to be available for a given system of interest, often necessitating contact with simulations *via* single-chain or full-fledged simulations and/or

SCPRISM. Despite these challenges, there are continued efforts to probe the ways in which PRISM can provide useful and accurate predictions for block copolymer systems.⁸²

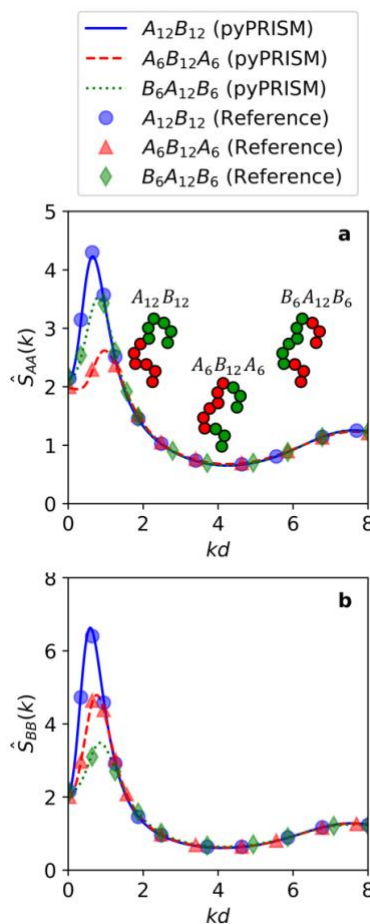


Figure 8: a) Collective partial structure factor between A (solvophilic) segments, $\hat{S}_{AA}(k)$, versus reduced wavenumber, kd , for amphiphilic A-B diblock, A-B-A triblock, and B-A-B triblock linear polymers as described in Figure 5 of Ref. 82. b) Collective partial structure factor between B (solvophobic) segments, $\hat{S}_{BB}(k)$, versus reduced wavenumber, kd , for amphiphilic A-B diblock, A-B-A triblock, and B-A-B triblock linear polymers as described in Figure 5 of Ref. 82. The total site density, ρ_{AB}^{site} , is ≈ 0.19 , and the strength of the B-B Lennard-Jones attraction is $\epsilon_{BB} = 0.25$. The lines are the predictions from pyPRISM and the symbols are data extracted from the corresponding referenced literature. In both subplots, $d = 1.0$ is the characteristic length scale of the system equal to the monomer site diameter. The details of how these data can be generated using pyPRISM can be found in the companion pyPRISM tutorial.¹⁹⁶

In Figure 8, we replicate recent results demonstrating how PRISM can be used to study the self-assembly of amphiphilic block copolymers in solution.⁸² Interestingly, while the previous block copolymer work using the Gaussian thread model necessitated *molecular* closures as described above,^{76, 227} an attractive bead-spring model in implicit solvent conditions showed agreement between molecular dynamics simulations and PRISM theory using the *atomic* PY closure.⁸² We plot the diagonal terms of the collective structure factor matrix, $\hat{S}_{AA}(k)$ and $\hat{S}_{BB}(k)$, in Figure 8a and 8b respectively, for three block copolymer sequences in which the A block is solvophilic and the B block is solvophobic: 1) A₁₂-B₁₂ diblock copolymer, 2) A₆-B₁₂-A₆ triblock copolymer, and 3) B₆-A₁₂-B₆ triblock copolymer. In this implicit solvent model system, A-A and A-B interactions are purely repulsive (described using the Weeks-Chandler-Andersen potential), while B-B interactions are described with an attractive Lennard-Jones potential. These interactions mimic the amphiphilic nature of the copolymer and B block solvophobicity, which induces micellization. The $\hat{w}(k)$ used in this work are obtained through single-chain molecular dynamics simulations and the Debye method, as analytical $\hat{w}(k)$ expressions are not readily available that span the range of block copolymer sequences, compositions, and degrees of solvophobicity studied. A-B diblock polymers show stronger A-A and B-B correlations than their triblock counterparts, and in the triblocks, correlations in the mid-blocks are stronger than correlations in the end-blocks. Furthermore, the location of the microphase peak maximum (k^*) provides information about the length scale of concentration fluctuations; the A-B diblocks have the lowest k^* , suggesting that A-B diblocks form larger micelles, and this inference was confirmed by the simulations.⁸² Finally, analyzing the trends in the $1/S_{BB}(k^*)$ as a function of B-B interaction strength allows for the prediction of the onset of micellization, as discussed in detail in Ref. ⁸².

D. General Challenges and Limitations

While the primary foci of this paper are the strengths and utility of PRISM theory, it is also important that we highlight some weaknesses and limitations associated with its use. As stated in the introduction, it is well known that using the classic, *atomic* closures to describe the phase behavior of polymer blends results in an incorrect scaling dependence of the spinodal temperature on chain length.⁶⁶ While correct scaling is recovered by using thermodynamic perturbation theory⁵⁰ or the *molecular closures*,^{52, 53} it is important to note that all closures are an inherent and unavoidable source of error in PRISM calculations due to the approximations invoked in their construction. For example, as true for even atomic liquids, both the HNC and PY closures have been shown to be thermodynamically inconsistent in that the system pressure calculated from separate virial, energetic, and compressibility routes is different.²²⁸ As stated in the approach section, *pyPRISM* helps users to assess the effect of the closure itself on the results by making it easy to switch between closures and/or implement new closures.

When using PRISM, users must recognize the classes of systems and states that are appropriate for the theory. The version of PRISM theory implemented in *pyPRISM* is a *liquid-state* theory for *isotropic, homogeneous* polymer liquids. PRISM cannot directly predict the structure of an ordered, macrophase-separated, or microphase-separated material. PRISM's foundation as a liquid-state theory also means that it is only applicable for systems with *liquid-like* structural correlations. While the exact definition of what is meant by liquid-like correlations is beyond the scope of this paper,²²⁸ this can generally be interpreted as an inability of PRISM theory to directly predict correlations for the glassy or crystalline states of polymer materials. On the other hand, many modern thermodynamic density functional theories for the spatially inhomogeneous

symmetry-broken state requires liquid state correlations as input, and PRISM theory is useful for this task.¹⁷⁴⁻¹⁷⁷

Compared to simulation methods like molecular dynamics or Monte Carlo, PRISM theory produces only pair correlation functions rather than a coordinate trajectory. This means that all results about structure and phase behavior must be inferred from the numerical analyses available from PRISM theory rather than direct visualization. While this is not a unique challenge to PRISM and is shared by other metrologies (*e.g.*, scattering, spectroscopy), the loss of visual analysis can be a difficult adjustment for those coming from a simulation background. Interestingly, self-consistent PRISM partially mitigates this problem by providing trajectories of single molecules in a mean-field, medium-induced solvation potential. While these trajectories do provide a physical picture of the molecular building blocks of a polymer system, they do not describe how the components interact with one another and suffer from limitations inherent in the mean-field treatment of the medium, as discussed above.

One of the challenges in solving the PRISM equations numerically is that the minimization functional (Equation 19) is extremely slow to converge and can be unstable with large fluctuations in Δ that can result from small changes in $\Gamma_{in}(r)$. The most important factor in determining the ability of *pyPRISM* to solve the PRISM equations is the quality of the initial guess $\Gamma_{in}(r)$ provided to the solver. Unfortunately, a guess for $\Gamma_{in}(r)$ is non-trivial to provide as it requires some knowledge of $C(r)$ and $H(r)$ *before* the PRISM equations are solved. A route towards producing improved guesses for $\Gamma_{in}(r)$ is to solve a system that is ‘*nearby*’ in phase or configuration space. For example, *pyPRISM* has difficulty converging for the N=100 case in Figure 6b using a guess of $\Gamma_{in}(r) = 0$, but can relatively easily converge for the N=2 000 case on the same guess. To solve for the shorter polymer system, we simply use the final Γ_{in} result from the N=2 000 solution as the

guess for $\Gamma_{in}(r)$ and *pyPRISM* converges. Similarly, the results for the D=16d diameter nanoparticles in Figure 7a cannot be directly solved from a naive initial guess but can be achieved iteratively by solving sequentially larger nanoparticles starting from D=1d. *pyPRISM* makes this process simple, as all details about the system and PRISM solution are held in memory and can easily be modified or utilized in a loop. For all examples shown this process is clearly laid out in the provided example scripts.

V. Summary

pyPRISM is an open-source Python framework that aims to reduce the barrier to using PRISM theory in the study of complex soft-matter based materials. While PRISM theory has been successfully applied to predict the equilibrium thermodynamic and structural behavior of a large array of soft-matter systems, its overall use has been limited compared to other simulation-techniques like molecular dynamics and Monte Carlo. While we cannot identify the exact reasons for this lack of use, it is likely related in part to the complexities involved in setting up and solving the PRISM formalism and issues associated with the closures as described in section IV.D. *pyPRISM* provides a straightforward interface to posing PRISM problems and data structures that simplify doing the mathematics associated with PRISM theory. Furthermore, by codifying our approach in an open-source package with both documentation and knowledgebase materials hosted on the repository web-site,¹⁹⁵⁻¹⁹⁷ we help to ensure that *pyPRISM* users produce correct and accurate results and provide a platform for users to easily contribute, create, and modify closures, numerical solution algorithms, and analyses. Overall, we hope that *pyPRISM* will nucleate a community of soft-material researchers that use PRISM theory to study, design, and understand novel polymer systems.

Acknowledgements:

TBM is supported by the NIST/NRC fellowship program and, in addition, this work has been supported by the members of the NIST *nSoft* consortium (nist.gov/nsoft). TEG and AJ thank NSF DMR-CMMT grant number 1609543 for financial support. This research was supported in part through the use of Information Technologies (IT) resources at the University of Delaware, specifically the high-performance computing resources of the Farber supercomputing cluster. This work used the Extreme Science and Engineering Discovery Environment (XSEDE) Stampede cluster at the University of Texas through allocation MCB100140 (AJ), which is supported by National Science Foundation grant number ACI-1548562. All authors thank Dr. Boualem Hammouda, Dr. Debra Audus, Dr. Ivan Lyubimov, Dr. Nils Persson, Jannat Nayem, and Dr. Ahmad Ghobadi for help with reviewing and developing this manuscript, documentation, and tutorial. Finally, all authors thank Prof. Kenneth Schweizer for his critical reading and valuable suggestions for improvement of this paper.

VI. References

1. Paolo, G.; Stefano, B.; Nicola, B.; Matteo, C.; Roberto, C.; Carlo, C.; Davide, C.; Guido, L. C.; Matteo, C.; Ismaila, D.; Andrea Dal, C.; Stefano de, G.; Stefano, F.; Guido, F.; Ralph, G.; Uwe, G.; Christos, G.; Anton, K.; Michele, L.; Layla, M.-S.; Nicola, M.; Francesco, M.; Riccardo, M.; Stefano, P.; Alfredo, P.; Lorenzo, P.; Carlo, S.; Sandro, S.; Gabriele, S.; Ari, P. S.; Alexander, S.; Paolo, U.; Renata, M. W. Quantum Espresso: A Modular and Open-Source Software Project for Quantum Simulations of Materials. *J. Phys.: Condens. Matter* **2009**, 21 (39), 395502
2. Gonze, X.; Jollet, F.; Abreu Araujo, F.; Adams, D.; Amadon, B.; Applencourt, T.; Audouze, C.; Beuken, J. M.; Bieder, J.; Bokhanchuk, A.; Bousquet, E.; Bruneval, F.; Caliste, D.; Côté, M.; Dahm, F.; Da Pieve, F.; Delaveau, M.; Di Gennaro, M.; Dorado, B.; Espejo, C.; Geneste, G.; Genovese, L.; Gerossier, A.; Giantomassi, M.; Gillet, Y.; Hamann, D. R.; He, L.; Jomard, G.; Laflamme Janssen, J.; Le Roux, S.; Levitt, A.; Lherbier, A.; Liu, F.; Lukačević, I.; Martin, A.; Martins, C.; Oliveira, M. J. T.; Poncé, S.; Pouillon, Y.; Rangel, T.; Rignanese, G. M.; Romero, A. H.; Rousseau, B.; Rubel, O.; Shukri, A. A.; Stankovski, M.; Torrent, M.; Van Setten, M. J.; Van Troeye, B.; Verstraete, M. J.; Waroquiers, D.; Wiktor, J.; Xu, B.; Zhou, A.; Zwanziger, J. W. Recent Developments in the Abinit Software Package. *Comput. Phys. Commun.* **2016**, 205, 106-131

3. Plimpton, S. Fast Parallel Algorithms for Short-Range Molecular-Dynamics. *J. Comput. Phys.* **1995**, 117 (1), 1-19
4. Berendsen, H. J. C.; Vanderspoel, D.; Vandrunen, R. Gromacs - a Message-Passing Parallel Molecular-Dynamics Implementation. *Comput. Phys. Commun.* **1995**, 91 (1-3), 43-56
5. Phillips, J. C.; Braun, R.; Wang, W.; Gumbart, J.; Tajkhorshid, E.; Villa, E.; Chipot, C.; Skeel, R. D.; Kalé, L.; Schulten, K. Scalable Molecular Dynamics with Namd. *J. Comput. Chem.* **2005**, 26 (16), 1781-1802
6. Anderson, J. A.; Lorenz, C. D.; Travesset, A. General Purpose Molecular Dynamics Simulations Fully Implemented on Graphics Processing Units. *J. Comput. Phys.* **2008**, 227 (10), 5342-5359
7. Smith, W.; Yong, C. W.; Rodger, P. M. Dl_Poly: Application to Molecular Simulation. *Mol. Simul.* **2002**, 28 (5), 385-471
8. Openmd: Molecular Dynamics in the Open. <http://openmd.org/> (October),
9. Eastman, P.; Swails, J.; Chodera, J. D.; McGibbon, R. T.; Zhao, Y.; Beauchamp, K. A.; Wang, L.-P.; Simmonett, A. C.; Harrigan, M. P.; Stern, C. D.; Wiewiora, R. P.; Brooks, B. R.; Pande, V. S. Openmm 7: Rapid Development of High Performance Algorithms for Molecular Dynamics. *PLoS Comput. Biol.* **2017**, 13 (7), e1005659
10. Arora, A.; Qin, J.; Morse, D. C.; Delaney, K. T.; Fredrickson, G. H.; Bates, F. S.; Dorfman, K. D. Broadly Accessible Self-Consistent Field Theory for Block Polymer Materials Discovery. *Macromolecules* **2016**, 49 (13), 4675-4690
11. Oof3d: Finite Element Analysis of Microstructures. <https://www.ctcms.nist.gov/oof/oof3d/> (October),
12. Multiphysics Object-Oriented Simulation Environment (Moose). <http://mooseframework.org/>. (October),
13. Alnæs, M.; Blechta, J.; Hake, J.; Johansson, A.; Kehlet, B.; Logg, A.; Richardson, C.; Ring, J.; Rognes, M. E.; Wells, G. N. The Fenics Project Version 1.5. *Archive of Numerical Software; Vol 3, No 100 (2015)* **2015**,
14. Martínez, L.; Andrade, R.; Birgin, E. G.; Martínez, J. M. Packmol: A Package for Building Initial Configurations for Molecular Dynamics Simulations. *J. Comput. Chem.* **2009**, 30 (13), 2157-2164
15. Hanwell, M. D.; Curtis, D. E.; Lonie, D. C.; Vandermeersch, T.; Zurek, E.; Hutchison, G. R. Avogadro: An Advanced Semantic Chemical Editor, Visualization, and Analysis Platform. *J. Cheminf.* **2012**, 4 (1), 17
16. Levine, B. G.; Stone, J. E.; Kohlmeyer, A. Fast Analysis of Molecular Dynamics Trajectories with Graphics Processing Units-Radial Distribution Function Histogramming. *J. Comput. Phys.* **2011**, 230 (9), 3556-3569
17. Michaud-Agrawal, N.; Denning, E. J.; Woolf, T. B.; Beckstein, O. Mdanalysis: A Toolkit for the Analysis of Molecular Dynamics Simulations. *J. Comput. Chem.* **2011**, 32 (10), 2319-2327
18. Humphrey, W.; Dalke, A.; Schulten, K. Vmd: Visual Molecular Dynamics. *J. Mol. Graph.* **1996**, 14 (1), 33-38
19. Alexander, S. Visualization and Analysis of Atomistic Simulation Data with Ovito—the Open Visualization Tool. *Modelling and Simulation in Materials Science and Engineering* **2010**, 18 (1), 015012

20. Ornstein, L. S.; Zernike, F. Accidental Deviations of Density and Opalescence at the Critical Point of a Simple Substance. *Proc. K. Akad. Wet.-Amsterdam* **1914**, 17, 793-806
21. Lowden, L. J.; Chandler, D. Solution of a New Integral-Equation for Pair Correlation-Functions in Molecular Liquids. *J. Chem. Phys.* **1973**, 59 (12), 6587-6595
22. Hsu, C. S.; Chandler, D. Rism Calculation of the Structure of Liquid Chloroform. *Mol. Phys.* **1979**, 37 (1), 299-301
23. Hsu, C. S.; Chandler, D. Rism Calculation of Structure of Liquid Acetonitrile. *Mol. Phys.* **1978**, 36 (1), 215-224
24. Hsu, C. S.; Chandler, D.; Lowden, L. J. Applications of Rism Equation to Diatomic Fluids - Liquids Nitrogen, Oxygen and Bromine. *Chem. Phys.* **1976**, 14 (2), 213-228
25. Schweizer, K. S.; Curro, J. G. Integral-Equation Theory of the Structure of Polymer Melts. *Phys. Rev. Lett.* **1987**, 58 (3), 246-249
26. Curro, J. G.; Schweizer, K. S. Theory of Polymer Melts - an Integral-Equation Approach. *Macromolecules* **1987**, 20 (8), 1928-1934
27. Honnell, K. G.; Curro, J. G.; Schweizer, K. S. Local-Structure of Semiflexible Polymer Melts. *Macromolecules* **1990**, 23 (14), 3496-3505
28. Schweizer, K. S.; Curro, J. G. Integral-Equation Theory of Polymer Melts - Intramolecular Structure, Local Order, and the Correlation Hole. *Macromolecules* **1988**, 21 (10), 3070-3081
29. Shew, C. Y.; Yethiraj, A. Self-Consistent Integral Equation Theory for Semiflexible Chain Polyelectrolyte Solutions. *J. Chem. Phys.* **2000**, 113 (19), 8841-8847
30. Khalatur, P. G.; Khokhlov, A. R. Hybrid Mc/Rism Technique for Simulation of Polymer Solutions: Monte Carlo Plus Rism Integral Equations. *Mol. Phys.* **1998**, 93 (4), 555-572
31. Melenkevitz, J.; Schweizer, K. S.; Curro, J. G. Self-Consistent Integral-Equation Theory for the Equilibrium Properties of Polymer-Solutions. *Macromolecules* **1993**, 26 (23), 6190-6196
32. Yethiraj, A.; Schweizer, K. S. Self-Consistent Polymer Integral-Equation Theory - Comparisons with Monte-Carlo Simulations and Alternative Closure Approximations. *J. Chem. Phys.* **1992**, 97 (2), 1455-1464
33. Schweizer, K. S.; Honnell, K. G.; Curro, J. G. Reference Interaction Site Model-Theory of Polymeric Liquids - Self-Consistent Formulation and Nonideality Effects in Dense Solutions and Melts. *J. Chem. Phys.* **1992**, 96 (4), 3211-3225
34. Li, H.; Curro, J. G.; Wu, D. T.; Habenschuss, A. X-Ray Scattering of Vinyl Polyolefin Liquids and Random Copolymers: Theory and Experiment. *Macromolecules* **2008**, 41 (7), 2694-2700
35. Habenschuss, A.; Tsighe, M.; Curro, J. G.; Grest, G. S.; Nath, S. K. Structure of Poly(Dialkylsiloxane) Melts: Comparisons of Wide-Angle X-Ray Scattering, Molecular Dynamics Simulations, and Integral Equation Theory. *Macromolecules* **2007**, 40 (19), 7036-7043
36. Curro, J. G.; Frischknecht, A. L. The Structure of Poly(Ethylene Oxide) Liquids: Comparison of Integral Equation Theory with Molecular Dynamics Simulations and Neutron Scattering. *Polymer* **2005**, 46 (17), 6500-6506
37. Sides, S. W.; Curro, J.; Grest, G. S.; Stevens, M. J.; Soddemann, T.; Habenschuss, A.; Londono, J. D. Structure of Poly(Dimethylsiloxane) Melts: Theory, Simulation, and Experiment. *Macromolecules* **2002**, 35 (16), 6455-6465

38. Putz, M.; Curro, J. G.; Grest, G. S. Self-Consistent Integral Equation Theory for Polyolefins: Comparison to Molecular Dynamics Simulations and X-Ray Scattering. *J. Chem. Phys.* **2001**, 114 (6), 2847-2860
39. Weinhold, J. D.; Curro, J. G.; Habenschuss, A.; Londono, J. D. Self-Consistent Integral Equation Theory of Polyolefins and Comparison to X-Ray Scattering Experiments. *Macromolecules* **1999**, 32 (21), 7276-7288
40. Pedersen, J. S.; Schurtenberger, P. Static Properties of Polystyrene in Semidilute Solutions: A Comparison of Monte Carlo Simulation and Small-Angle Neutron Scattering Results. *Europhys. Lett.* **1999**, 45 (6), 666-672
41. Zirkel, A.; Gruner, S. M.; Urban, V.; Thiyagarajan, P. Small-Angle Neutron Scattering Investigation of the Q-Dependence of the Flory-Huggins Interaction Parameter in a Binary Polymer Blend. *Macromolecules* **2002**, 35 (19), 7375-7386
42. Tillman, P. A.; Rottach, D. R.; McCoy, J. D.; Plimpton, S. J.; Curro, J. G. The Structure and Thermodynamics of Energetically and Structurally Asymmetric Polymer Blends. *J. Chem. Phys.* **1998**, 109 (2), 806-814
43. Gromov, D. G.; de Pablo, J. J. Phase Equilibria in Binary Polymer Blends: Integral Equation Approach. *J. Chem. Phys.* **1998**, 109 (22), 10042-10052
44. Weinhold, J. D.; Kumar, S. K.; Singh, C.; Schweizer, K. S. Athermal Stiffness Blends - a Comparison of Monte-Carlo Simulations and Integral-Equation Theory. *J. Chem. Phys.* **1995**, 103 (21), 9460-9474
45. Stevenson, C. S.; McCoy, J. D.; Plimpton, S. J.; Curro, J. G. Molecular-Dynamics Simulations of Athermal Polymer Blends - Finite System Size Considerations. *J. Chem. Phys.* **1995**, 103 (3), 1200-1207
46. Stevenson, C. S.; Curro, J. G.; McCoy, J. D.; Plimpton, S. J. Molecular-Dynamics Simulations of Athermal Polymer Blends - Comparison with Integral-Equation Theory. *J. Chem. Phys.* **1995**, 103 (3), 1208-1215
47. Singh, C.; Schweizer, K. S.; Yethiraj, A. Fluctuation Phenomena in Structurally Symmetrical Polymer Blends. *J. Chem. Phys.* **1995**, 102 (5), 2187-2208
48. Singh, C.; Schweizer, K. S. Correlation-Effects and Entropy-Driven Phase-Separation in Athermal Polymer Blends. *J. Chem. Phys.* **1995**, 103 (13), 5814-5832
49. Schweizer, K. S.; Singh, C. Microscopic Solubility-Parameter Theory of Polymer Blends - General Predictions. *Macromolecules* **1995**, 28 (6), 2063-2080
50. Rajasekaran, J. J.; Curro, J. G.; Honeycutt, J. D. Theory for the Phase-Behavior of Polyolefin Blends - Application to the Polyethylene/Isotactic Polypropylene Blend. *Macromolecules* **1995**, 28 (20), 6843-6853
51. Kumar, S. K.; Yethiraj, A.; Schweizer, K. S.; Leermakers, F. A. M. The Effects of Local Stiffness Disparity on the Surface Segregation from Binary Polymer Blends. *J. Chem. Phys.* **1995**, 103 (23), 10332-10346
52. Yethiraj, A.; Schweizer, K. S. Integral-Equation Theory of Polymer Blends - Numerical Investigation of Molecular Closure Approximations. *J. Chem. Phys.* **1993**, 98 (11), 9080-9093
53. Schweizer, K. S.; Yethiraj, A. Polymer Reference Interaction Site Model-Theory - New Molecular Closures for Phase-Separating Fluids and Alloys. *J. Chem. Phys.* **1993**, 98 (11), 9053-9079

54. Schweizer, K. S. Analytic Rism Theory of Polymer Alloys - Molecular Closure Predictions for Structurally Symmetrical Blends. *Macromolecules* **1993**, 26 (22), 6033-6049
55. Schweizer, K. S. Analytic Prism Theory of Structurally Asymmetric Polymer Blends and Copolymers. *Macromolecules* **1993**, 26 (22), 6050-6067
56. Honeycutt, J. D. Applications of Polymer Rism Theory to Blends. *Makromol. Chem., Macromol. Symp.* **1993**, 65, 49-57
57. Yethiraj, A.; Schweizer, K. S. On the Scaling of the Critical-Temperature with the Degree of Polymerization in Symmetrical Polymer Blends. *J. Chem. Phys.* **1992**, 97 (8), 5927-5930
58. Schweizer, K. S.; Curro, J. G. Analytic Reference Interaction Site Model-Mean Spherical Approximation-Theory of Flexible Polymer Blends - Effects of Spatial and Fractal Dimensions. *J. Chem. Phys.* **1991**, 94 (5), 3986-4000
59. Curro, J. G.; Schweizer, K. S. Integral-Equation Theory for Compressible Polymer Alloys - Thermodynamics, Scattering, and Miscibility of Gaussian Chains. *Macromolecules* **1991**, 24 (25), 6736-6747
60. Schweizer, K. S.; Curro, J. G. Rism Theory of Polymer Liquids - Analytical Results for Continuum Models of Melts and Alloys. *Chem. Phys.* **1990**, 149 (1-2), 105-127
61. Schweizer, K. S.; Curro, J. G. Integral-Equation Theory of Polymer Blends. *Mol. Cryst. Liq. Cryst.* **1990**, 180, 69-76
62. Curro, J. G.; Schweizer, K. S. An Integral-Equation Theory of Polymer Blends - Athermal Mixtures. *Macromolecules* **1990**, 23 (5), 1402-1411
63. Schweizer, K. S.; Curro, J. G. Integral-Equation Theory of the Structure and Thermodynamics of Polymer Blends. *J. Chem. Phys.* **1989**, 91 (8), 5059-5081
64. Schweizer, K. S.; Curro, J. G. Microscopic Theory of the Structure, Thermodynamics, and Apparent X-Parameter of Polymer Blends. *Phys. Rev. Lett.* **1988**, 60 (9), 809-812
65. Curro, J. G.; Schweizer, K. S. Theory for the Chi Parameter of Polymer Blends - Effect of Attractive Interactions. *J. Chem. Phys.* **1988**, 88 (11), 7242-7243
66. Deutsch, H. P.; Binder, K. Evidence against the Integral-Equation Theory of Polymer Blends. *Europhys. Lett.* **1992**, 17 (8BIS), 697-702
67. Heine, D. R.; Grest, G. S.; Curro, J. G., Structure of Polymer Melts and Blends: Comparison of Integral Equation Theory and Computer Simulations. In *Advanced Computer Simulation Approaches for Soft Matter Sciences I*, Holm, C., Kremer, K., Eds. 2005; Vol. 173, pp 209-249.
68. Tillman, P. A.; Rottach, D. R.; McCoy, J. D.; Plimpton, S. J.; Curro, J. G. The Effect of Attractions on the Structure and Thermodynamics of Model Polymer Blends. *J. Chem. Phys.* **1997**, 107 (10), 4024-4032
69. Heine, D.; Wu, D. T.; Curro, J. G.; Grest, G. S. Role of Intramolecular Energy on Polyolefin Miscibility: Isotactic Polypropylene/Polyethylene Blends. *The Journal of Chemical Physics* **2003**, 118 (2), 914-924
70. Cabral, J. T.; Higgins, J. S. Small Angle Neutron Scattering from the Highly Interacting Polymer Mixture Tmpc/Psd: No Evidence of Spatially Dependent Chi Parameter. *Macromolecules* **2009**, 42 (24), 9528-9536
71. Hall, L. M.; Schweizer, K. S. Impact of Monomer Sequence, Composition and Chemical Heterogeneity on Copolymer-Mediated Effective Interactions between Nanoparticles in Melts. *Macromolecules* **2011**, 44 (8), 3149-3160

72. Sung, B. J.; Yethiraj, A. Integral Equation Theory of Randomly Coupled Multiblock Copolymer Melts: Effect of Block Size on the Phase Behavior. *J. Chem. Phys.* **2005**, 123 (21),
73. Sung, B. J.; Yethiraj, A. Integral Equation Theory of Random Copolymer Melts: Self-Consistent Treatment of Intramolecular and Intermolecular Correlations. *J. Chem. Phys.* **2005**, 122 (23),
74. Sung, B. J.; Yethiraj, A. Integral Equation Theory of Random Copolymer Melts. *Macromolecules* **2005**, 38 (5), 2000-2008
75. Makeeva, I. V.; Talitskikh, S. K.; Khalatur, P. G. Structure Formation in a System of Regular Multiblock Copolymers: Integral Equation Theory. *Polym. Sci. Ser. A* **2001**, 43 (12), 1297-1304
76. Guenza, M.; Schweizer, K. S. Fluctuations Effects in Diblock Copolymer Fluids: Comparison of Theories and Experiment. *J. Chem. Phys.* **1997**, 106 (17), 7391-7410
77. David, E. F.; Schweizer, K. S. Liquid State Theory of Thermally Driven Segregation of Conformationally Asymmetric Diblock Copolymer Melts. *Macromolecules* **1997**, 30 (17), 5118-5132
78. David, E. F.; Schweizer, K. S. Solvent-Mediated Interactions and Chain Conformations in Block-Copolymer Liquids. *J. Chem. Soc.-Faraday Trans.* **1995**, 91 (16), 2411-2425
79. David, E. F.; Schweizer, K. S. Influence of Conformational Asymmetries on Local Packing and Small-Angle Scattering in Athermal Diblock Copolymer Melts. *Macromolecules* **1995**, 28 (11), 3980-3994
80. David, E. F.; Schweizer, K. S. Integral-Equation Theory of Block-Copolymer Liquids .1. General Formalism and Analytic Predictions for Symmetrical Copolymers. *J. Chem. Phys.* **1994**, 100 (10), 7767-7783
81. David, E. F.; Schweizer, K. S. Integral-Equation Theory of Block-Copolymer Liquids .2. Numerical Results for Finite Hard-Core Diameter Chains. *J. Chem. Phys.* **1994**, 100 (10), 7784-7795
82. Lyubimov, I.; Beltran-Villegas, D. J.; Jayaraman, A. Prism Theory Study of Amphiphilic Block Copolymer Solutions with Varying Copolymer Sequence and Composition. *Macromolecules* **2017**, 50 (18), 7419-7431
83. Modica, K. J.; Martin, T. B.; Jayaraman, A. Effect of Polymer Architecture on the Structure and Interactions of Polymer Grafted Particles: Theory and Simulations. *Macromolecules* **2017**, 50 (12), 4854-4866
84. Martin, T. B.; Jayaraman, A. Using Theory and Simulations to Calculate Effective Interactions in Polymer Nanocomposites with Polymer-Grafted Nanoparticles. *Macromolecules* **2016**, 49 (24), 9684-9692
85. Sankar, U. K.; Tripathy, M. Dispersion, Depletion, and Bridging of Athermal and Attractive Nanorods in Polymer Melt. *Macromolecules* **2015**, 48 (2), 432-442
86. Xu, Q. Z.; Xu, M. J.; Feng, Y. C.; Chen, L. Structure and Effective Interactions of Comb Polymer Nanocomposite Melts. *J. Chem. Phys.* **2014**, 141 (20),
87. Ganesan, V.; Jayaraman, A. Theory and Simulation Studies of Effective Interactions, Phase Behavior and Morphology in Polymer Nanocomposites. *Soft Matter* **2014**, 10 (1), 13-38
88. Xu, M. J.; Zhao, Q. L.; Zhang, C.; Du, Z. J.; Mi, J. G. Integral Equation Prediction of Surface-Induced Layering Transition of Polymer Nanocomposites. *J. Phys. Chem. C* **2013**, 117 (38), 19409-19418

89. Martin, T. B.; Jayaraman, A. Polydisperse Homopolymer Grafts Stabilize Dispersions of Nanoparticles in a Chemically Identical Homopolymer Matrix: An Integrated Theory and Simulation Study. *Soft Matter* **2013**, 9 (29), 6876-6889
90. Martin, T. B.; Dodd, P. M.; Jayaraman, A. Polydispersity for Tuning the Potential of Mean Force between Polymer Grafted Nanoparticles in a Polymer Matrix. *Phys. Rev. Lett.* **2013**, 110 (1), 018301
91. Kim, S. Y.; Zukoski, C. F. Molecular Weight Effects on Particle and Polymer Microstructure in Concentrated Polymer Solutions. *Macromolecules* **2013**, 46 (16), 6634-6643
92. Banerjee, D.; Dadmun, M.; Sumpter, B.; Schweizer, K. S. Theory of the Miscibility of Fullerenes in Random Copolymer Melts. *Macromolecules* **2013**, 46 (21), 8732-8743
93. Jayaraman, A.; Nair, N. Integrating Prism Theory and Monte Carlo Simulation to Study Polymer-Functionalised Particles and Polymer Nanocomposites. *Mol. Simul.* **2012**, 38 (8-9), 751-761
94. Nair, N.; Wentzel, N.; Jayaraman, A. Effect of Bidispersity in Grafted Chain Length on Grafted Chain Conformations and Potential of Mean Force between Polymer Grafted Nanoparticles in a Homopolymer Matrix. *J. Chem. Phys.* **2011**, 134 (19),
95. Kim, S. Y.; Schweizer, K. S.; Zukoski, C. F. Multiscale Structure, Interfacial Cohesion, Adsorbed Layers, and Thermodynamics in Dense Polymer-Nanoparticle Mixtures. *Phys. Rev. Lett.* **2011**, 107 (22),
96. Frischknecht, A. L.; Yethiraj, A. Two- and Three-Body Interactions among Nanoparticles in a Polymer Melt. *J. Chem. Phys.* **2011**, 134 (17),
97. Nair, N.; Jayaraman, A. Self-Consistent Prism Theory-Monte Carlo Simulation Studies of Copolymer Grafted Nanoparticles in a Homopolymer Matrix. *Macromolecules* **2010**, 43 (19), 8251-8263
98. Hall, L. M.; Schweizer, K. S. Structure, Scattering Patterns and Phase Behavior of Polymer Nanocomposites with Nonspherical Fillers. *Soft Matter* **2010**, 6 (5), 1015-1025
99. Hall, L. M.; Jayaraman, A.; Schweizer, K. S. Molecular Theories of Polymer Nanocomposites. *Curr. Opin. Solid State Mater. Sci.* **2010**, 14 (2), 38-48
100. Frischknecht, A. L.; McGarrity, E. S.; Mackay, M. E. Expanded Chain Dimensions in Polymer Melts with Nanoparticle Fillers. *J. Chem. Phys.* **2010**, 132 (20),
101. Jayaraman, A.; Schweizer, K. S. Effective Interactions and Self-Assembly of Hybrid Polymer Grafted Nanoparticles in a Homopolymer Matrix. *Macromolecules* **2009**, 42 (21), 8423-8434
102. Jayaraman, A.; Schweizer, K. S. Liquid State Theory of the Structure and Phase Behaviour of Polymer-Tethered Nanoparticles in Dense Suspensions, Melts and Nanocomposites. *Mol. Simul.* **2009**, 35 (10-11), 835-848
103. Hall, L. M.; Anderson, B. J.; Zukoski, C. F.; Schweizer, K. S. Concentration Fluctuations, Local Order, and the Collective Structure of Polymer Nanocomposites. *Macromolecules* **2009**, 42 (21), 8435-8442
104. Jayaraman, A.; Schweizer, K. S. Effective Interactions, Structure, and Phase Behavior of Lightly Tethered Nanoparticles in Polymer Melts. *Macromolecules* **2008**, 41 (23), 9430-9438
105. Jayaraman, A.; Schweizer, K. S. Effect of the Number and Placement of Polymer Tethers on the Structure of Concentrated Solutions and Melts of Hybrid Nanoparticles. *Langmuir* **2008**, 24 (19), 11119-11130

106. Jayaraman, A.; Schweizer, K. S. Structure and Assembly of Dense Solutions and Melts of Single Tethered Nanoparticles. *J. Chem. Phys.* **2008**, 128 (16),
107. Hall, L. M.; Schweizer, K. S. Many Body Effects on the Phase Separation and Structure of Dense Polymer-Particle Melts. *J. Chem. Phys.* **2008**, 128 (23),
108. Zhao, L.; Li, Y. G.; Zhong, C. L. Integral Equation Theory Study on the Phase Separation in Star Polymer Nanocomposite Melts. *J. Chem. Phys.* **2007**, 127 (15),
109. Zhao, L.; Li, Y. G.; Zhong, C. L. Integral Equation Theory Study on the Structure and Effective Interactions in Star Polymer Nanocomposite Melts. *J. Chem. Phys.* **2007**, 126 (1),
110. Sen, S.; Xie, Y. P.; Kumar, S. K.; Yang, H. C.; Bansal, A.; Ho, D. L.; Hall, L.; Hooper, J. B.; Schweizer, K. S. Chain Conformations and Bound-Layer Correlations in Polymer Nanocomposites. *Phys. Rev. Lett.* **2007**, 98 (12),
111. Zhao, L.; Li, Y. G.; Zhong, C.; Mi, J. Structure and Effective Interactions in Polymer Nanocomposite Melts: An Integral Equation Theory Study. *J. Chem. Phys.* **2006**, 124 (14),
112. Hooper, J. B.; Schweizer, K. S. Theory of Phase Separation in Polymer Nanocomposites. *Macromolecules* **2006**, 39 (15), 5133-5142
113. Hooper, J. B.; Schweizer, K. S. Contact Aggregation, Bridging, and Steric Stabilization in Dense Polymer-Particle Mixtures. *Macromolecules* **2005**, 38 (21), 8858-8869
114. Hooper, J. B.; Schweizer, K. S.; Desai, T. G.; Koshy, R.; Koblinski, P. Structure, Surface Excess and Effective Interactions in Polymer Nanocomposite Melts and Concentrated Solutions. *J. Chem. Phys.* **2004**, 121 (14), 6986-6997
115. Doxastakis, M.; Chen, Y. L.; Guzman, O.; de Pablo, J. J. Polymer-Particle Mixtures: Depletion and Packing Effects. *J. Chem. Phys.* **2004**, 120 (19), 9335-9342
116. Chatterjee, A. P.; Schweizer, K. S. Microscopic Theory of Polymer-Mediated Interactions between Spherical Particles. *J. Chem. Phys.* **1998**, 109 (23), 10464-10476
117. Chatterjee, A. P.; Schweizer, K. S. Correlation Effects in Dilute Particle-Polymer Mixtures. *J. Chem. Phys.* **1998**, 109 (23), 10477-10488
118. Yethiraj, A.; Hall, C. K.; Dickman, R. Interaction between Colloids in Solutions Containing Dissolved Polymer. *J. Colloid Interface Sci.* **1992**, 151 (1), 102-117
119. Chervanyov, A. I. Effect of Attractive Interactions between Polymers on the Effective Force Acting between Colloids Immersed in a Polymer System: Analytic Liquid-State Theory. *J. Chem. Phys.* **2016**, 145 (24),
120. Banerjee, D.; Yang, J.; Schweizer, K. S. Entropic Depletion in Colloidal Suspensions and Polymer Liquids: Role of Nanoparticle Surface Topography. *Soft Matter* **2015**, 11 (47), 9086-9098
121. Pelaez-Fernandez, M.; Moncho-Jorda, A.; Callejas-Fernandez, J. Charged Colloid-Polymer Mixtures: A Study on Electrostatic Depletion Attraction. *J. Chem. Phys.* **2011**, 134 (5),
122. Pelaez-Fernandez, M.; Moncho-Jorda, A.; Callejas-Fernandez, J. Structure of Charged Colloid-Polymer Mixtures. *Epl* **2010**, 90 (4),
123. Costa, D.; Hansen, J. P.; Harnau, L. Structure and Equation of State of Interaction Site Models for Disc-Shaped Lamellar Colloids. *Mol. Phys.* **2005**, 103 (14), 1917-1927
124. Chen, Y. L.; Schweizer, K. S. Liquid-State Theory of Structure, Thermodynamics, and Phase Separation in Suspensions of Rod Polymers and Hard Spheres. *J. Phys. Chem. B* **2004**, 108 (21), 6687-6696

125. Shah, S. A.; Ramakrishnan, S.; Chen, Y. L.; Schweizer, K. S.; Zukoski, C. F. Scattering Studies of the Structure of Colloid-Polymer Suspensions and Gels. *Langmuir* **2003**, 19 (12), 5128-5136
126. Ramakrishnan, S.; Fuchs, M.; Schweizer, K. S.; Zukoski, C. F. Concentration Fluctuations in a Model Colloid-Polymer Suspension: Experimental Tests of Depletion Theories. *Langmuir* **2002**, 18 (4), 1082-1090
127. Ramakrishnan, S.; Fuchs, M.; Schweizer, K. S.; Zukoski, C. F. Entropy Driven Phase Transitions in Colloid-Polymer Suspensions: Tests of Depletion Theories. *J. Chem. Phys.* **2002**, 116 (5), 2201-2212
128. Harnau, L.; Hansen, J. P. Colloid Aggregation Induced by Oppositely Charged Polyions. *J. Chem. Phys.* **2002**, 116 (20), 9051-9057
129. Fuchs, M.; Schweizer, K. S. Structure of Colloid-Polymer Suspensions. *J. Phys.-Condes. Matter* **2002**, 14 (12), R239-R269
130. Shusharina, N. P.; Khalatur, P. G.; Khokhlov, A. R. Phase Behavior of Polymer Containing Colloidal Dispersions: The Integral Equation Theory. *J. Chem. Phys.* **2000**, 113 (16), 7006-7012
131. Josef, E.; Bianco-Peled, H. Conformation of a Natural Polyelectrolyte in Semidilute Solutions with No Added Salt. *Soft Matter* **2012**, 8 (35), 9156-9165
132. Yethiraj, A. Liquid State Theory of Polyelectrolyte Solutions. *J. Phys. Chem. B* **2009**, 113 (6), 1539-1551
133. Zherenkova, L. V.; Komarov, P. V.; Khalatur, P. G. Effective Intramolecular Interactions in Weakly Charged Polyelectrolytes: Relation to Structural Behavior of Solution. *Polym. Sci. Ser. A* **2006**, 48 (8), 859-869
134. Winkler, R. G. Structure of Polyelectrolyte Solutions: Influence of Salt and Chain Flexibility. *Macromol. Symp.* **2004**, 211, 55-70
135. Zherenkova, L. V.; Khalatur, P. G.; Khokhlov, A. R. Solution Properties of Charged Quasi-Random Copolymers: Integral Equation Theory. *J. Chem. Phys.* **2003**, 119 (13), 6959-6972
136. Hofmann, T.; Winkler, R. G.; Reineker, P. Influence of Salt on the Structure of Polyelectrolyte Solutions: An Integral Equation Theory Approach. *J. Chem. Phys.* **2003**, 119 (4), 2406-2413
137. Hofmann, T.; Winkler, R. G.; Reineker, P. Self-Consistent Integral Equation Theory for Solutions of Finite Extensible Semiflexible Polyelectrolyte Chains. *J. Chem. Phys.* **2003**, 118 (14), 6624-6633
138. Shew, C. Y.; Yethiraj, A. Integral Equation Theory for the Structure of DNA Solutions. *J. Chem. Phys.* **2002**, 116 (12), 5308-5314
139. Shew, C. Y.; Yethiraj, A. The Effect of Acid-Base Equilibria on the Fractional Charge and Conformational Properties of Polyelectrolyte Solutions. *J. Chem. Phys.* **2001**, 114 (6), 2830-2838
140. Hofmann, T.; Winkler, R. G.; Reineker, P. Integral Equation Theory Approach to Rodlike Polyelectrolytes: Counterion Condensation. *J. Chem. Phys.* **2001**, 114 (22), 10181-10188
141. Shew, C. Y.; Yethiraj, A. Computer Simulations and Integral Equation Theory for the Structure of Salt-Free Rigid Rod Polyelectrolyte Solutions: Explicit Incorporation of Counterions. *J. Chem. Phys.* **1999**, 110 (23), 11599-11607

142. Shew, C. Y.; Yethiraj, A. Monte Carlo Simulations and Self-Consistent Integral Equation Theory for Polyelectrolyte Solutions. *J. Chem. Phys.* **1999**, 110 (11), 5437-5443
143. Patra, C. N.; Yethiraj, A. Density Functional Theory for the Distribution of Small Ions around Polyions. *J. Phys. Chem. B* **1999**, 103 (29), 6080-6087
144. Dymitrowska, M.; Belloni, L. Integral Equation Theory of Flexible Polyelectrolytes. II. Primitive Model Approach. *J. Chem. Phys.* **1999**, 111 (14), 6633-6642
145. Dymitrowska, M.; Belloni, L. Integral Equation Theory of Flexible Polyelectrolytes. I. Debye-Huckel Approach. *J. Chem. Phys.* **1998**, 109 (11), 4659-4669
146. Yethiraj, A. Conformational Properties and Static Structure Factor of Polyelectrolyte Solutions. *Phys. Rev. Lett.* **1997**, 78 (19), 3789-3792
147. Shew, C. Y.; Yethiraj, A. Integral Equation Theory of Solutions of Rigid Polyelectrolytes. *J. Chem. Phys.* **1997**, 106 (13), 5706-5719
148. Yethiraj, A.; Shew, C. Y. Structure of Polyelectrolyte Solutions. *Phys. Rev. Lett.* **1996**, 77 (18), 3937-3940
149. Belloni, L.; Delacruz, M. O.; Delsanti, M.; Dalbiez, J. P.; Spalla, O.; Drifford, M. Polyelectrolyte Solutions Plus Multivalent Salts = Phase-Separation. *Nuovo Cimento Soc. Ital. Fis. D-Condens. Matter At. Mol. Chem. Phys. Fluids Plasmas Biophys.* **1994**, 16 (7), 727-736
150. Hirata, F.; Levy, R. M. Salt-Induced Conformational-Changes in DNA - Analysis Using the Polymer Rism Theory. *J. Phys. Chem.* **1989**, 93 (1), 479-484
151. Patil, R.; Schweizer, K. S.; Chang, T. M. Stretching, Packing, and Thermodynamics in Highly Branched Polymer Melts. *Macromolecules* **2003**, 36 (7), 2544-2552
152. Yethiraj, A. Integral Equation Theory for the Surface Segregation from Blends of Linear and Star Polymers. *Comput. Theor. Polym. Sci.* **2000**, 10 (1-2), 115-123
153. Duda, Y.; Garcia, I.; Trokhymchuk, A.; Henderson, D. The Correlations in a Star Molecule Fluid. Integral Equation Theory and Monte Carlo Study. *Mol. Phys.* **2000**, 98 (17), 1287-1293
154. Grayce, C. J.; Schweizer, K. S. A Liquid-State Theory of Dense Star Polymer Fluids. *Macromolecules* **1995**, 28 (22), 7461-7478
155. Xu, Q. Z.; Feng, Y. C.; Chen, L. Phase Separation of Comb Polymer Nanocomposite Melts. *Soft Matter* **2016**, 12 (5), 1385-1400
156. Bolisetty, S.; Rosenfeldt, S.; Rochette, C. N.; Harnau, L.; Lindner, P.; Xu, Y.; Muller, A. H. E.; Ballauff, M. Interaction of Cylindrical Polymer Brushes in Dilute and Semi-Dilute Solution. *Colloid Polym. Sci.* **2009**, 287 (2), 129-138
157. Bolisetty, S.; Airaud, C.; Xu, Y.; Muller, A. H. E.; Harnau, L.; Rosenfeldt, S.; Lindner, P.; Ballauff, M. Softening of the Stiffness of Bottle-Brush Polymers by Mutual Interaction. *Phys. Rev. E* **2007**, 75 (4),
158. Khalatur, P. G.; Khokhlov, A. R. Phase Behavior of Comblike Copolymers: The Integral Equation Theory. *J. Chem. Phys.* **2000**, 112 (10), 4849-4861
159. Yethiraj, A.; Curro, J. G.; Rajasekaran, J. J. Thermodynamics and Local-Structure of Vinyl Polymer Melts. *J. Chem. Phys.* **1995**, 103 (6), 2229-2236
160. Honeycutt, J. D. A Theoretical-Study of Tacticity Effects on Poly(Vinyl Chloride) Poly(Methyl Methacrylate) Miscibility. *Macromolecules* **1994**, 27 (19), 5377-5381
161. Curro, J. G. Intermolecular Structure and Thermodynamics of Vinyl Polymer Liquids - Freely-Jointed Chains. *Macromolecules* **1994**, 27 (17), 4665-4672

162. Harnau, L.; Rosenfeldt, S.; Ballauff, M. Structure Factor and Thermodynamics of Rigid Dendrimers in Solution. *J. Chem. Phys.* **2007**, 127 (1),
163. Rosenfeldt, S.; Karpuk, E.; Lehmann, M.; Meier, H.; Lindner, P.; Harnau, L.; Ballauff, M. The Solution Structure of Stilbenoid Dendrimers: A Small-Angle Scattering Study. *ChemPhysChem* **2006**, 7 (10), 2097-2104
164. Choi, E.; Yethiraj, A. Conformational Properties of a Polymer in an Ionic Liquid: Computer Simulations and Integral Equation Theory of a Coarse-Grained Model. *J. Phys. Chem. B* **2015**, 119 (29), 9091-9097
165. Zherenkova, L. V.; Komarov, P. V. Study of the Phase Behavior of a Diblock Copolymer in an Ionic Liquid: Outlook for Use of the Integral-Equation Theory. *Polym. Sci. Ser. A* **2014**, 56 (3), 383-392
166. Zherenkova, L. V.; Komarov, P. V.; Belov, A. N.; Pavlov, A. S. A Polymer in an Ionic Liquid: Effect of the Length of the Cationic Nonpolar Tail on the Character of Interchain Correlations. *Polym. Sci. Ser. A* **2012**, 54 (2), 147-154
167. Oyerokun, F. T.; Schweizer, K. S. Theory of Glassy Dynamics in Conformationally Anisotropic Polymer Systems. *J. Chem. Phys.* **2005**, 123 (22),
168. Oyerokun, F. T.; Schweizer, K. S. Thermodynamics, Orientational Order and Elasticity of Strained Liquid Crystalline Melts and Elastomers. *J. Phys. Chem. B* **2005**, 109 (14), 6595-6603
169. Pickett, G. T.; Schweizer, K. S. Liquid Crystallinity in Flexible and Rigid Rod Polymers. *J. Chem. Phys.* **2000**, 112 (10), 4881-4892
170. Pickett, G. T.; Schweizer, K. S. Liquid-State Theory of Anisotropic Flexible Polymer Fluids. *J. Chem. Phys.* **1999**, 110 (14), 6597-6600
171. Yethiraj, A. Molecular Modeling of Polymers at Surfaces. *Chem. Eng. J.* **1999**, 74 (1-2), 109-115
172. Yethiraj, A.; Hall, C. K. Integral-Equation Theory for the Adsorption of Chain Fluids in Slitlike Pores. *J. Chem. Phys.* **1991**, 95 (5), 3749-3755
173. Schweizer, K. S.; Fuchs, M.; Szamel, G.; Guenza, M.; Tang, H. Polymer-Mode-Coupling Theory of the Slow Dynamics of Entangled Macromolecular Fluids. *Macromol. Theory Simul.* **1997**, 6 (6), 1037-1117
174. Patra, C. N.; Yethiraj, A. Density Functional Theory for Nonuniform Polymers: Accurate Treatment of the Effect of Attractive Interactions. *J. Chem. Phys.* **2003**, 118 (10), 4702-4706
175. Frischknecht, A. L.; Weinhold, J. D.; Salinger, A. G.; Curro, J. G.; Frink, L. J. D.; McCoy, J. D. Density Functional Theory for Inhomogeneous Polymer Systems. I. Numerical Methods. *J. Chem. Phys.* **2002**, 117 (22), 10385-10397
176. Frischknecht, A. L.; Curro, J. G.; Frink, L. J. D. Density Functional Theory for Inhomogeneous Polymer Systems. II. Application to Block Copolymer Thin Films. *J. Chem. Phys.* **2002**, 117 (22), 10398-10411
177. Donley, J. P.; Rajasekaran, J. J.; McCoy, J. D.; Curro, J. G. Microscopic Approach to Inhomogeneous Polymeric Liquids. *J. Chem. Phys.* **1995**, 103 (12), 5061-5069
178. Wang, Q.; Yang, D. The Recent Structure-Based Coarse Graining of Polymer Melts Using Prism Theory Does Not Give Thermodynamic Consistency. *Polymer* **2017**, 111, 103-106

179. Wang, Q. Systematic and Simulation-Free Coarse Graining of Multi-Component Polymeric Systems: Structure-Based Coarse Graining of Binary Polymer Blends. *Polymer* **2017**, 117, 315-330
180. Dinpajoo, M.; Guenza, M. G. On the Density Dependence of the Integral Equation Coarse-Graining Effective Potential. *J. Phys. Chem. B.* **2017**,
181. Dinpajoo, M.; Guenza, M. G. Thermodynamic Consistency in the Structure-Based Integral Equation Coarse-Grained Method. *Polymer* **2017**, 117, 282-286
182. Yang, D. L.; Wang, Q. Systematic and Simulation-Free Coarse Graining of Homopolymer Melts: A Structure-Based Study. *J. Chem. Phys.* **2015**, 142 (5),
183. Yang, D. L.; Wang, Q. Systematic and Simulation-Free Coarse Graining of Homopolymer Melts: A Relative-Entropy-Based Study. *Soft Matter* **2015**, 11 (36), 7109-7118
184. Guenza, M. G.; Iop, Structural and Thermodynamic Consistency in Coarse-Grained Models of Macromolecules. In *Xxvi Iupap Conference on Computational Physics*, 2015; Vol. 640.
185. Clark, A. J.; McCarty, J.; Guenza, M. G. Comment on “Systematic and Simulation-Free Coarse Graining of Homopolymer Melts: A Structure-Based Study” [J. Chem. Phys. 142, 054905 (2015)]. *J. Chem. Phys* **2015**, 143 (6), 067101
186. McCarty, J.; Clark, A. J.; Copperman, J.; Guenza, M. G. An Analytical Coarse-Graining Method Which Preserves the Free Energy, Structural Correlations, and Thermodynamic State of Polymer Melts from the Atomistic to the Mesoscale. *J. Chem. Phys.* **2014**, 140 (20),
187. Clark, A. J.; McCarty, J.; Guenza, M. G. Effective Potentials for Representing Polymers in Melts as Chains of Interacting Soft Particles. *J. Chem. Phys.* **2013**, 139 (12),
188. McCarty, J.; Clark, A. J.; Lyubimov, I. Y.; Guenza, M. G. Thermodynamic Consistency between Analytic Integral Equation Theory and Coarse-Grained Molecular Dynamics Simulations of Homopolymer Melts. *Macromolecules* **2012**, 45 (20), 8482-8493
189. Mullinax, J. W.; Noid, W. G. A Generalized-Yvon-Born-Green Theory for Determining Coarse-Grained Interaction Potentials. *J. Phys. Chem. C* **2010**, 114 (12), 5661-5674
190. Clark, A. J.; Guenza, M. G. Mapping of Polymer Melts onto Liquids of Soft-Colloidal Chains. *J. Chem. Phys.* **2010**, 132 (4),
191. Sambriski, E. J.; Guenza, M. G. Theoretical Coarse-Graining Approach to Bridge Length Scales in Diblock Copolymer Liquids. *Phys. Rev. E* **2007**, 76 (5),
192. Yatsenko, G.; Sambriski, E. J.; Nemirovskaya, M. A.; Guenza, M. Analytical Soft-Core Potentials for Macromolecular Fluids and Mixtures. *Phys. Rev. Lett.* **2004**, 93 (25),
193. Schulz, M.; Frisch, H. L.; Reineker, P. An Analytic Percus-Yevick Approach to the Rism Model of Monodisperse, Homopolymer Melts. *New J. Phys.* **2004**, 6,
194. Krakoviack, V.; Rotenberg, B.; Hansen, J. P. An Integral Equation Approach to Effective Interactions between Polymers in Solution. *J. Phys. Chem. B* **2004**, 108 (21), 6697-6706
195. Martin, T. B.; Gartner III, T. E. Pyprism Documentation. <http://pyprism.readthedocs.io>
196. Martin, T. B.; Gartner III, T. E. Pyprism Tutorial. <http://pyprism.readthedocs.io/en/latest/tutorial/tutorial.html>
197. Martin, T. B.; Gartner III, T. E. Pyprism Package. <http://github.com/usnistgov/pyPRISM>
198. Any Identification of Commerical or Open-Source Software in This Paper Is Done So Purely in Order to Specify the Methodology Adequately. Such Identification Is Not Intended to Imply Recommendation or Endorsement by the National Institute of

- Standards and Technology, nor Is It Intended to Imply That the Softwares Identified Are Necessarily the Best Available for the Purpose.
199. Schweizer, K. S.; Curro, J. G., Integral Equation Theories of the Structure, Thermodynamics, and Phase Transitions of Polymer Fluids. In *Advances in Chemical Physics, Vol 98*, Prigogine, I., Rice, S. A., Eds. 1997; Vol. 98, pp 1-142.
 200. Schweizer, K. S.; Curro, J. G., Prism Theory of the Structure, Thermodynamics, and Phase-Transitions of Polymer Liquids and Alloys. In *Atomistic Modeling of Physical Properties*, Monnerie, L., Suter, U. W., Eds. 1994; Vol. 116, pp 319-377.
 201. Hansen, J.-P.; McDonald, I. R., Theory of Simple Liquids. In *Theory of Simple Liquids (Fourth Edition)*, Academic Press: Oxford, 2013.
 202. McCoy, J. D.; Honnell, K. G.; Curro, J. G.; Schweizer, K. S.; Honeycutt, J. D. Single-Chain Structure in Model Polyethylene Melts. *Macromolecules* **1992**, 25 (19), 4905-4910
 203. Honnell, K. G.; McCoy, J. D.; Curro, J. G.; Schweizer, K. S.; Narten, A. H.; Habenschuss, A. Local-Structure of Polyethylene Melts. *J. Chem. Phys.* **1991**, 94 (6), 4659-4662
 204. Chen, W. R.; Butler, P. D.; Magid, L. J. Incorporating Intermicellar Interactions in the Fitting of SANS Data from Cationic Wormlike Micelles. *Langmuir* **2006**, 22 (15), 6539-6548
 205. Pedersen, J. S.; Schurtenberger, P. Scattering Functions of Semidilute Solutions of Polymers in a Good Solvent. *J. Polym. Sci. Pt. B-Polym. Phys.* **2004**, 42 (17), 3081-3094
 206. Arleth, L.; Bauer, R.; Øgendal, L. H.; Egelhaaf, S. U.; Schurtenberger, P.; Pedersen, J. S. Growth Behavior of Mixed Wormlike Micelles: A Small-Angle Scattering Study of the Lecithin–Bile Salt System. *Langmuir* **2003**, 19 (10), 4096-4104
 207. Arleth, L.; Bergstrom, M.; Pedersen, J. S. Small-Angle Neutron Scattering Study of the Growth Behavior, Flexibility, and Intermicellar Interactions of Wormlike Sds Micelles in NaBr Aqueous Solutions. *Langmuir* **2002**, 18 (14), 5343-5353
 208. Flory, P. J., *Statistical Mechanics of Chain Molecules*. John Wiley & Sons, Inc.: 1969.
 209. Jones, E.; Oliphant, E.; Peterson, P. <http://www.scipy.org/>
 210. Martin, T. B.; Jayaraman, A. Effect of Matrix Bidispersity on the Morphology of Polymer-Grafted Nanoparticle-Filled Polymer Nanocomposites. *J. Polym. Sci. Pt. B-Polym. Phys.* **2014**, 52 (24), 1661-1668
 211. Tsige, M.; Curro, J. G.; Grest, G. S. Packing of Poly(Tetrafluoroethylene) in the Liquid State: Molecular Dynamics Simulation and Theory. *J. Chem. Phys.* **2008**, 129 (21),
 212. Sung, B. J.; Yethiraj, A. Monte Carlo Simulation and Self-Consistent Integral Equation Theory for Polymers in Quenched Random Media. *J. Chem. Phys.* **2005**, 123 (7),
 213. Mendez, S.; Curro, J. G.; Putz, M.; Bedrov, D.; Smith, G. D. Explicit Inclusion of the Solvent Molecules. *J. Chem. Phys.* **2001**, 115 (12), 5669-5678
 214. Vasilevskaya, V. V.; Khalatur, P. G.; Khokhlov, A. R. Conformation of a Polymer Chain near the Solvent Critical Region. 1. The Integral Equation Theory. *J. Chem. Phys.* **1998**, 109 (12), 5108-5118
 215. Grayce, C. J.; Yethiraj, A.; Schweizer, K. S. Liquid-State Theory of the Density-Dependent Conformation of Nonpolar Linear-Polymers. *J. Chem. Phys.* **1994**, 100 (9), 6857-6872
 216. Walt, S. v. d.; Colbert, S. C.; Varoquaux, G. The Numpy Array: A Structure for Efficient Numerical Computation. *Comput. Sci. Eng.* **2011**, 13 (2), 22-30
 217. Oliphant, T. E. Python for Scientific Computing. *Comput. Sci. Eng.* **2007**, 9 (3), 10-20

218. Zhao, L.; Li, Y. G.; Mi, J. G.; Zhong, C. L. Integral Equation Theory for Atactic Polystyrene Melt with a Coarse-Grained Model. *J. Chem. Phys.* **2005**, 123 (12),
219. Freischmidt, H. M.; Shanks, R. A.; Moad, G.; Uhlherr, A. Characterization of Polyolefin Melts Using the Polymer Reference Interaction Site Model Integral Equation Theory with a Single-Site United Atom Model. *J. Polym. Sci. Pt. B-Polym. Phys.* **2001**, 39 (16), 1803-1814
220. Curro, J. G.; Webb, E. B.; Grest, G. S.; Weinhold, J. D.; Putz, M.; McCoy, J. D. Comparisons between Integral Equation Theory and Molecular Dynamics Simulations for Realistic Models of Polyethylene Liquids. *J. Chem. Phys.* **1999**, 111 (19), 9073-9081
221. Xu, Q. Z.; Mi, J. G.; Zhong, C. L. Integral Equation Theory for Gas Sorption and Swelling of Glassy Atactic Polystyrene. *Ind. Eng. Chem. Res.* **2010**, 49 (10), 4914-4922
222. Budzien, J. L.; McCoy, J. D.; Curro, J. G.; LaViolette, R. A.; Peterson, E. S. The Solubility of Gases in Polyethylene: Integral Equation Study of Standard Molecular Models. *Macromolecules* **1998**, 31 (19), 6669-6675
223. Curro, J. G.; Schweizer, K. S. Integral-Equation Theory of Homopolymer Melts. *Mol. Cryst. Liq. Cryst.* **1990**, 180, 77-89
224. Halverson, J. D.; Lee, W. B.; Grest, G. S.; Grosberg, A. Y.; Kremer, K. Molecular Dynamics Simulation Study of Nonconcatenated Ring Polymers in a Melt. I. Statics. *J. Chem. Phys.* **2011**, 134 (20), 204904
225. Schweizer, K. S.; Curro, J. G. Equation of State of Polymer Melts - General Formulation of a Microscopic Integral-Equation Theory. *J. Chem. Phys.* **1988**, 89 (5), 3342-3349
226. Schweizer, K. S.; Curro, J. G. Equation of State of Polymer Melts - Numerical Results for Athermal Freely Jointed Chain Fluids. *J. Chem. Phys.* **1988**, 89 (5), 3350-3362
227. Guenza, M.; Schweizer, K. S. Local and Microdomain Concentration Fluctuation Effects in Block Copolymer Solutions. *Macromolecules* **1997**, 30 (14), 4205-4219
228. Hansen, J.-P.; McDonald, I. R., Chapter 4 - Distribution Function Theories. In *Theory of Simple Liquids (Fourth Edition)*, Academic Press: Oxford, 2013; pp 105-147.